Geological Quarterly, 2025, 69, 31
DOI: https://doi.org/10.7306/gq.1804

Potential mineral resources of the Moon

Tadeusz A. PRZYLIBSKI[1, *], Mateusz SZCZĘŚNIEWICZ[1] and Konrad BLUTSTEIN[2]

[1] Wrocław University of Science and Technology, Faculty of Geoengineering, Mining and Geology, Laboratory of Geology and Mineral Engineering, Wybrzeże S. Wyspiańskiego 27, 50-370 Wrocław, Poland; ORCID: 0000-0002-8094-7944 [T.A.P.], 0000-0003-2006-7950 [M.Sz.]

[2] Graduate of the Wrocław University of Science and Technology, Faculty of Geoengineering, Mining and Geology, doctor of the team's alumni of the Laboratory of Geology and Mineral Engineering, Wybrzeże S. Wyspiańskiego 27, Wrocław, Poland; ORCID: 0000-0003-1337-774X [K.B.]

Przylibski, T.A., Szczęśniewicz, M., Blutstein, K., 2025. Potential mineral resources of the Moon. Geological Quarterly, 69, 31; https://doi.org/10.7306/gq.1804

Associate Editor: Stanisław Wołkowicz

Higlights:
– The most geochemically and geophysically evolved layer is the regolith;
– Lunar regolith should be treated as a multi-component, pre-crushed ore;
– The first object of exploitation and processing on the Moon will be regolith;
– Potential deposit zones include outcrops of ultrabasic igneous rocks enriched in metals: Cr, Ti, REE, and PGM;
– The most promising deposit areas are the lunar maria, primarily the Procellarum KREEP Terrane, circumpolar areas, and regions on the far side with a regolith thickness > 10 m.

The homogeneity of the chemical and isotopic compositions of the Earth and the Moon facilitates the identification of potential mineral resources present and exploitable on the Moon. Current knowledge of the geological structure of the Moon indicates that the greatest geochemical and geophysical activity of the surface layer of the Moon's crust lies in the regolith, and it is this that promises the most promising lunar raw material resource base. The regolith contains increased concentrations of life-supporting raw materials (H_2O and O_2), fuels and energy raw materials (^3He, U, Th, H_2, and O_2), metallic raw materials (Fe, Ti, Zr, Hf, Eu, other REEs, Cr, Ni, Co, Al, and Si), rock raw materials (regolith, breccias, basalts, anorthosites, and others) and chemical raw materials (K, P, Cl, and S). Lunar regolith should be treated as a multi-component, pre-crushed ore, in which there are local enrichments of selected raw materials, and so initially will form the target of exploitation and processing on the Moon. The next potential deposit zones are outcrops of basic and ultrabasic igneous rocks, which may be enriched in metals such as Cr, Ti, REEs and PGMs, or places where these rocks are covered by only a thin layer of regolith. Such zones also include areas of occurrence of acidic igneous rocks, enriched in quartz, and perhaps also in many other valuable metals and chemical raw materials. The most important prospective areas in terms of the occurrence of raw materials in the regolith are the lunar maria, primarily the Procellarum KREEP Terrane, circumpolar areas, as well as areas on the far side of the Moon characterized by a regolith thickness exceeding 10 m.

Key words: lunar regolith, lunar resources, extraterrestrial resources, space resources, KREEP basalts, lunar maria.

INTRODUCTION

The Moon, the Earth's only natural satellite, is, next to Mars, the main target of upcoming space missions and a potential place to create the first bases for permanent human residence outside our planet. With a diameter of 3,475 km, it is the fourth largest natural satellite in the Solar System. The average distance of the Moon from Earth is only 384,400 km, or less than 1.3 light-sec (Mutch, 1972). This significantly reduces future transport or travel costs, and also facilitates communication and remote operation of probes, rovers, mining and construction machines, navigation, observation, and communication systems. It is also a relatively well-known extraterrestrial object due to centuries of astronomical observations and, above all, due to the manned space missions of the Apollo program and the unmanned missions of the Luna and Chang'e programs, which brought samples of lunar rocks and regolith to Earth. Recently, progress in collecting information about the Moon's geological structure has been accelerating due to remote sensing data provided by lunar satellites (the American Lunar Reconnaissance Orbiter and the Indian Chandrayaan-2). Much important data is also provided by the burgeoning study of lunar meteorites, which are being found on Earth in rapidly increasing numbers and mass, due to intensive searches in cold and hot deserts (Przylibski et al., 2023; MetBull, 2023). All these features mean that we can treat the Moon as not only the closest

* Corresponding author, e-mail: Tadeusz.Przylibski@pwr.edu.pl

Received: April 18, 2025; accepted: July 16, 2025; first published online: October 13, 2025

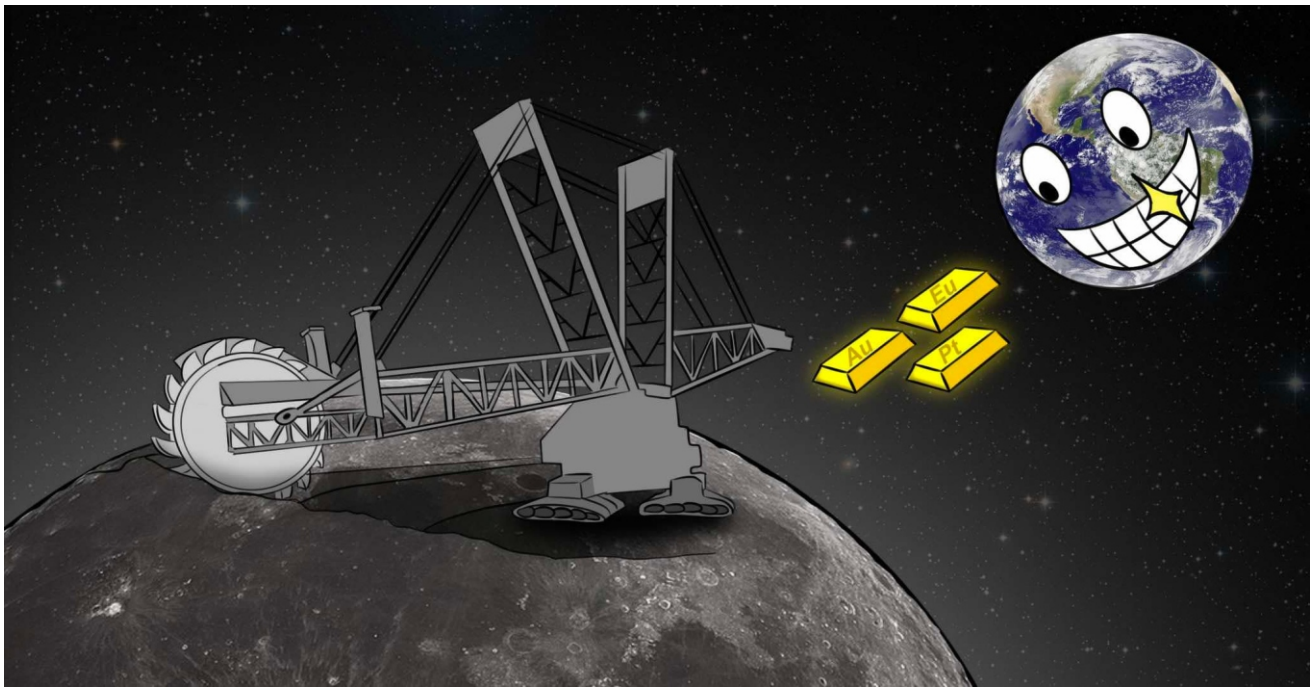

Graphical abstract

celestial body to Earth but as a potential source of useful raw materials for the development of our civilization (Przylibski et al., 2024). In the context of the Moon, we can think both about the *in situ* use of raw materials (SRU or ISRU – Space Resource Utilization or In Situ Resource Utilization; Anand et al., 2012; Schwandt et al., 2012; Bennett et al., 2020; Hadler et al., 2020; Rasera et al., 2020), and about supplying the Earth with strategic, critical raw materials (Blutstein, 2021). Currently, research on the Moon is well enough advanced to allow us to determine the potential raw materials to be found on its surface, and even estimate their perspective resources.

Here, we explore the most promising raw materials of which exploitation will be possible (and most likely necessary) on the surface of the Moon, and describe the characteristics and genesis of the deposits of these raw materials, their location, and potential resources. We provide a comprehensive new assessment of contemporary knowledge on the occurrence of natural resources and their deposit accumulations in the surface layers of the Moon. The new data we present include the estimated resources of the most important raw materials in the lunar regolith.

ORIGIN OF THE MOON

The canonical model of the origin of the Moon, or the giant-impact hypothesis, associates the formation of Earth's natural satellite with the collision of two planetary embryos (protoplanets) during the late stages of the early evolution of the Solar System, when planetary accretion took place. According to this model, the proto-Earth experienced an oblique collision with a hypothetical protoplanet called Theia, an object about the size of modern Mars. As a result of this collision, silicate-rich material with a mass slightly greater than the current mass of the Moon was ejected into the orbit of the proto-Earth. This material then formed a disc. However, according to the canonical model, much of the material in the disk came from the impactor, which was Theia. Over the course of several hundred to thousands of years after the collision, the disk material cooled, condensed, and moved beyond the Roche limit. Beyond this limit, gravitational tidal forces are small enough to allow the accretion of material to form the Moon (Barr, 2016).

The weakness of the canonical model is its inability to explain the observed homogeneity of the chemical (and isotopic) compositions of the Earth and the Moon (Barr, 2016). Therefore, another model was sought that would explain this homogeneity, that is, a mechanism leading to the mixing of the components of proto-Earth and Theia. Such a model must also consider that most of the angular momentum of the Earth-Moon system should be concentrated in the Moon, as is currently observed. The concentration of as much as 1.2% of the mass and 80% of the angular momentum in the Moon makes our natural satellite and the Earth-Moon system unique in the entire Solar System (Barr, 2016).

The most recently proposed model for the formation of the Moon following an off-centre collision between Theia and proto-Earth is the synestia theory (Lock et al., 2018). A synestia is a new type of planetary structure formed from completely vaporized protoplanets involved in a collision. It has the shape of a swollen cloud resembling a thick doughnut, which is thicker on the outside than on the inside. At this outer edge of the cloud, vaporized rock circulates so rapidly that the cloud takes on a new structure, with a thick disk orbiting the inner region. As the model shows, the disk does not separate from the central region, allowing for the material within it to be thoroughly mixed. Cooling of the synestia drives the mixing of material from both bodies involved in the collision, and condensation generates the formation and growth of moons orbiting within the synestia's outer part. As a result, the Moon equalizes its isotopic and chemical composition with the material forming the synestia and, in about a year, through the accretion of condensing material, reaches its final size and mass. Then, over the next several decades, the cooling synestia decreases in size. This causes the Moon to separate from the synestia, ending the main stage of lunar accretion and causing the Moon to finally solidify and cool. The remainder of the synestia continues to cool and solidify within the Roche limit until the planet (Earth) forms. According to this model, giant impacts that produce potential synestias, including the one that formed the Moon and Earth, were common towards the end of the formation of terrestrial planets in the young Solar System (Lock et al., 2018).

However, there is still no single, universally accepted model for the formation of the Moon. Research is ongoing to expand the canonical model based on the collision of the proto-Earth with Theia (Zhou et al., 2024), and new concepts are being introduced. One such new concept is the formation of massive terrestrial satellites through binary-exchange capture (Williams and Zugger, 2024). This concept explores the possibility of satellite capture from the process of collision-less binary exchange and shows that massive satellites in the range 0.01–0.1 Earth mass can be captured by Earth-sized terrestrial planets in a way already demonstrated for larger planets in the solar system. The number of concepts based on computer modeling will likely continue to grow, but many are being rejected due to the difficulty of explaining the large portion of the Earth-Moon system's angular momentum concentrated in the Moon, the relatively large mass of the Moon, as well as the difficulty of explaining the identical elemental and isotopic composition of both bodies. This last observed fact requires very thorough mixing of Earth and Moon matter, which is not achieved in many computer impact models. In this respect, the synestia model has many advantages.

SKETCH OF THE MOON'S GEOLOGY

The modern Moon, like the Earth, is a differentiated body in hydrodynamic equilibrium, and nearly spherical in shape, with a radius of 1,737 km. It is composed of three concentric spheres: the crust, the mantle, and the core. The outermost crust is on average 49 ±16 km thick. It is thicker on the far side and thinner on the near side, which causes the centre of mass to be shifted relative to the geometric centre of the Moon. The mantle is over 1,350 km thick and is the source of deep moonquakes. The upper mantle is rich in pyroxenes, while the lower part of the Moon's mantle may be partially molten and consists of Mg-rich olivines forming cumulates, probably the first product of crystallization of the magma ocean. Geophysical data indicate that the core is composed of a small solid inner core and a liquid outer core with a radius of 330 km (Taylor and McLennan, 2010; Jaumann et al., 2012).

The Moon's crust is a single plate that has been subjected to only slight internal stress. The lunar highlands are a unique example in the solar system of a body covered with a primordial crust formed by anorthosites crystallizing from a magma ocean (Taylor and McLennan, 2010). The Moon's crust and underlying mantle are divided into distinct terranes, even though its evolution was not affected by plate tectonics. Terranes have been distinguished based on their unique geochemical, geophysical and geological properties. The greater concentration of radioactive elements in the Procellarum KREEP Terrane (PKT) on the near side of the Moon, which produce heat in nuclear transformation processes, led to the near side of the Moon being more volcanically active than the far side. Within the PKT there are basalts with increased Th content in the range of 3–12 ppm. This terrane includes the Oceanus Procellarum (Ocean of Storms) and the Mare Imbrium (Sea of Rains). The largest lunar terrane is the Feldspathic Highlands Terrane (FHT), covering ~60% of the Moon's surface. The main rocks in this terrane are iron-enriched anorthosites. The third major terrane is the oldest and largest of all lunar basins, the South Pole-Aitken (SPA). In addition to these three large terranes, a fourth terrane has been described, the Eastern Basin Terrane (EBT; Jaumann at al., 2012).

The lunar crust is composed of four main rock types (anorthosites, basalts, regolith) in terms of geochemical diversity and the results of mechanical destruction and mixing of mineral components. About 99% of the Moon's surface is made up of rocks older than 3 Ga and over 80% of the rocks are older than 4 Ga (Taylor and McLennan, 2010).

Four main processes are involved in the formation of the Moon's surface: collisions with space objects (impacts), volcanism, tectonics, and space weathering caused by the impact of solar wind particles, as well as UV and X-ray radiation on rock surfaces (Melosh, 2011; Jaumann et al., 2012; Kallio et al., 2019). During the oldest eon in the history of the Moon (Eolunarian; >4.3 Ga), endogenic processes, including solidification of the magma ocean, were dominant. Anorthosites, KREEP rocks and magnesium facies rocks crystallized at that time. During the second, younger eon (Paleolunarian; 4.3–3.16 Ga) endogenic processes (mainly magmatism – plutonism – crystallization of residual magma and volcanism – basalt eruptions that filled the lunar maria) and exogenic processes (impacts with variously sized meteoroids and asteroids) were of similar importance. As the Moon's interior cooled, the scale of endogenic processes decreased significantly (rare basaltic lava flows), which meant that exogenic processes played an increasingly important role in shaping the surface, resulting in the formation of craters and sediment covers created by the material ejected from them. This period covers the third, youngest eon (Neolunarian), which lasts from 3.16 Ga to the present (Greeley and Batson, 1999; Ji et al., 2022).

The first rock types that make up the Moon's crust are the rocks that make up the highlands. These are iron-rich anorthosites, which constitute 80% of the crust of the lunar highlands. The age of their crystallization from the magma ocean is estimated at 4.460 ±0.400 Ga (Greeley and Batson, 1999; Taylor and McLennan, 2010; Jaumann et al., 2012). KREEP rocks also occur within the primitive crust. These were formed as a result of crystallization of the residual melt, which constitutes ~2% of the original magma. This residual melt contained a particularly large amount of incompatible trace elements, which is why these rocks are highly enriched in REEs – by a factor of a thousand relative to CI-type carbonaceous chondrites, and are also enriched in potassium and phosphorus, as well as in uranium and thorium. The KREEP rocks were the last product of crystallization of the magma ocean. Their age is estimated at ~4.36 Ga (4.35–4.39 Ga; Borg et al., 2015). These rocks do not form a continuous layer; they occur almost exclusively on the near side of the Moon in the form of lenses and pods (Greeley and Batson, 1999; Taylor and McLennan, 2010; Jaumann et al., 2012). The last formation of igneous abyssal rocks comprises the rocks of the magnesium facies (Mg-suite rocks). These rocks constitute a maximum of ~10% of the volume of the Moon's crust, and appear on the near side. They are spatially associated with the KREEP rocks and are probably the product of crystallization of magma which was a mixture of KREEP magma with other, more primitive magma. These include troctolites, spinel troctolites, norites, gabbronorites and dunites. Their age is 4.44–4.20 Ga (Greeley and Batson, 1999; Taylor and McLennan, 2010; Jaumann et al., 2012). The latest research results suggest that their age is 4.33 ±0.02 Ga (Zhang et al., 2021).

The second type of rocks that make up the younger, secondary crust of the Moon are basaltic volcanic rocks enriched in FeO and TiO_2 and depleted in Al_2O_3, which form the lunar maria regions. The maria cover ~17% (Jaumann et al., 2012) of the Moon's surface and are mostly located on the near side. The thickness of the basalt cover varies from several hundred metres to 4 km in the centers of circular 'seas', e.g. Mare Imbrium. Typically, the basalt cover is thinner than 500 m. Lunar mare basalts originate from independent eruptions from different sources at different depths and flood (fill) the nearest ac-

cessible depressions. The source of magmas are local zones in the lunar mantle unrelated to surface structures. The absence of basalt maria in the Moon's far side is due to the greater thickness of the crust. Most lunar basalts are the product of partial melting of a non-tholeiitic, anhydrous basalt source region located at various depths (of the order of 200–400 km) at temperatures of ~1200°C (Taylor and McLennan, 2010). The melting was probably caused by local concentrations of radioactive isotopes of U, Th, and ^{40}K. Diffuse sources of basaltic magmas cause their considerable diversity in chemical and mineral composition. We currently are able to distinguish around 25 types of lunar basalt. This is due to fractional crystallization near the surface, but is also undoubtedly the effect of local variations in the chemical composition of the mantle. The age of the oldest basalts is estimated at 4.3–3.9 Ga, while the youngest, rare basalts are only 1 Ga. Compared to terrestrial basalts, the lunar basalts are depleted in SiO_2 (containing 37–45%), but are enriched in FeO (containing 18–22%); they are also enriched in Ti, Cr, and the K/U ratio in them is 2500, more than 4 times less than in terrestrial basalts (10,000–12,500; Greeley and Batson, 1999; Taylor and McLennan, 2010; Jaumann et al., 2012).

The next two types of rocks are associated with exogenic processes at the lunar surface. These include the third type of lunar crustal rocks, which are clastic breccias formed as a result of one or more meteoroid and asteroid impacts on the lunar surface. They form a mixture of different rock types. The Moon experienced its strongest bombardment between the collisions of Nectaris (3.92 Ga) and Imbrium (3.85 Ga) – during the Nectarian Period (Taylor and McLennan, 2010).

The surface of the lunar crust is formed by a fourth type of lunar crust rock – an unconsolidated layer of fine-grained rubble called regolith, which contains crystalline fragments of rocks and minerals bonded together by glass produced during micrometeorite impacts (regolith breccias). The outermost, surface part of the regolith with the finest grains is called lunar soil (Jaumann et al., 2012). The thickness of the regolith is in the range of 2–14 m, although there are local accumulations in which the regolith layer exceeds 14 m in thickness (Jin et al., 2010; Papike et al., 1982). On the Moon's near side, the thickness of the regolith is <10 m, while on the far side it locally reaches >10 m (Carrier et al., 1991; Jin et al., 2010). The average diameter of regolith particles ranges from ~60 to ~80 μm (Melosh, 2011; Jaumann et al., 2012), while the median diameter of regolith particles ranges from 40 to 130 μm with a mean of 70 μm (Carrier et al., 1991). The composition of the regolith is dominated by mineral fragments, clasts of unaltered crystalline rock, fragments of breccia, glass, and agglutinates – fragments of rocks and minerals stuck together with glass. There is also meteoritic material, which may constitute up to 2% of the volume of the regolith (Melosh, 2011; Jaumann et al., 2012). At the surface, the density of the regolith is 1,400 kg/m^3, but at a depth of 1 m it increases to 2,000 kg/m^3 (Melosh, 2011; Jaumann et al., 2012), and according to the latest measurements at the Chang'e 3 landing site, the bulk density increases from 850 kg/m^3 at the surface to 2,250 kg/m^3 at a depth of 5 m (Fa, 2020). The composition of the regolith is dominated by local material, although ~10% of the regolith consists of particles (ejecta) transported from great distances by powerful collisions of asteroids and meteoroids with the lunar surface (Melosh, 2011; Jaumann et al., 2012; Kallio et al., 2019). Regolith is estimated to be accumulating on the lunar surface at a rate of ~1.5 mm per 1 Myr (Taylor and McLennan, 2010). A cross-section through the lunar regolith is shown in Figure 1. The current summary of the physico-chemical, mineralogical, petrological and genetic characteristics of the regolith can be found in the review of Qin et al. (2025).

This development of the Moon's geological structure requires looking for potential deposits of mineral resources in the surface layer, the regolith. This layer is composed of rocks that have experienced and continue to experience the greatest geochemical and geophysical changes. Due to this, minerals and chemical elements can be "sorted" in them, ultimately creating accumulations that can be treated as their deposits. Regolith is undoubtedly the most promising source of diverse natural resources, especially in comparison to the mostly very old igneous rocks that make up the Moon's crust, which have not been subject to intense alteration by geochemical (and physical) processes after their formation.

RESOURCES OF THE MOON AND THEIR POTENTIAL DEPOSITS

The Moon's crust represents a type of the primordial planetary crust formed on the first planets in the young Solar System. This crust was only slightly subject to the processes of geochemical differentiation (Taylor and McLennan, 2010; Jaumann et al., 2012). As a result, the Moon may appear to be poor in deposits of various natural resources. The formation of accumulations (deposits) of raw materials is usually associated with chemical reactions and with processes in which elements are selected with respect to their density, volatility, melting and crystallization temperature, atomic mass, ionic radius, electrons structure, electron affinity, ionization energy and other physicochemical properties (Gruszczyk, 1984; Smirnow, 1986; Polański, 1988; Migaszewski and Gałuszka, 2007). However, the surface of the Moon's crust has been subject to certain geochemical and geophysical processes over the past billion years. It has been transformed by exogenic processes, mainly impact metamorphism caused by the fall of asteroids, meteoroids, micrometeoroids and interplanetary dust particles onto the surface. The surface materials constituting the lunar regolith have also been subjected to space weathering processes, i.e. the impact of cosmic radiation and solar wind particles (Johnson et al., 1999; McLennan, 2010; Melosh, 2011; Jaumann et al., 2012; He et al., 2023). Although these processes were only able to transform the lunar regolith to a small extent, even their non-intensive but long-term action led to the concentration of useful natural resources, which we can call deposits (Johnson et al., 1999; McLennan, 2010; Melosh, 2011; Jaumann et al., 2012; He et al., 2023). Therefore, we consider that that the regolith is the most important rock layer of the Moon, and that it contains perspective deposits of various raw materials (Fig. 1). Additionally, this layer is strongly crushed (or even ground) and fragmented, which further facilitates the extraction of individual raw materials from it. Therefore, as with asteroids (Łuszczek and Przylibski, 2019, 2021), the regolith should be treated as a layer containing the most accessible deposits of raw materials. Raw materials from lunar regolith are the easiest to extract and exploit due to the lowest possible energy consumption of the processes of mining the already fragmented rock, as well as its significant enrichment in the desired raw material. Due to this, the exploitation of regolith deposits will be the least technically and technologically complicated, as well as the cheapest (Łuszczek and Przylibski, 2019, 2021; Przylibski et al., 2022).

Of all the raw materials present on the Moon, the most fundamental are undoubtedly the ones necessary to sustain life. This applies especially to the raw materials necessary to supply permanent human bases on the Moon. Initially, these will be scientific bases, for example those designed in the Artemis program currently implemented by the National Aeronautics and Space Administration (NASA), and over time probably industrial

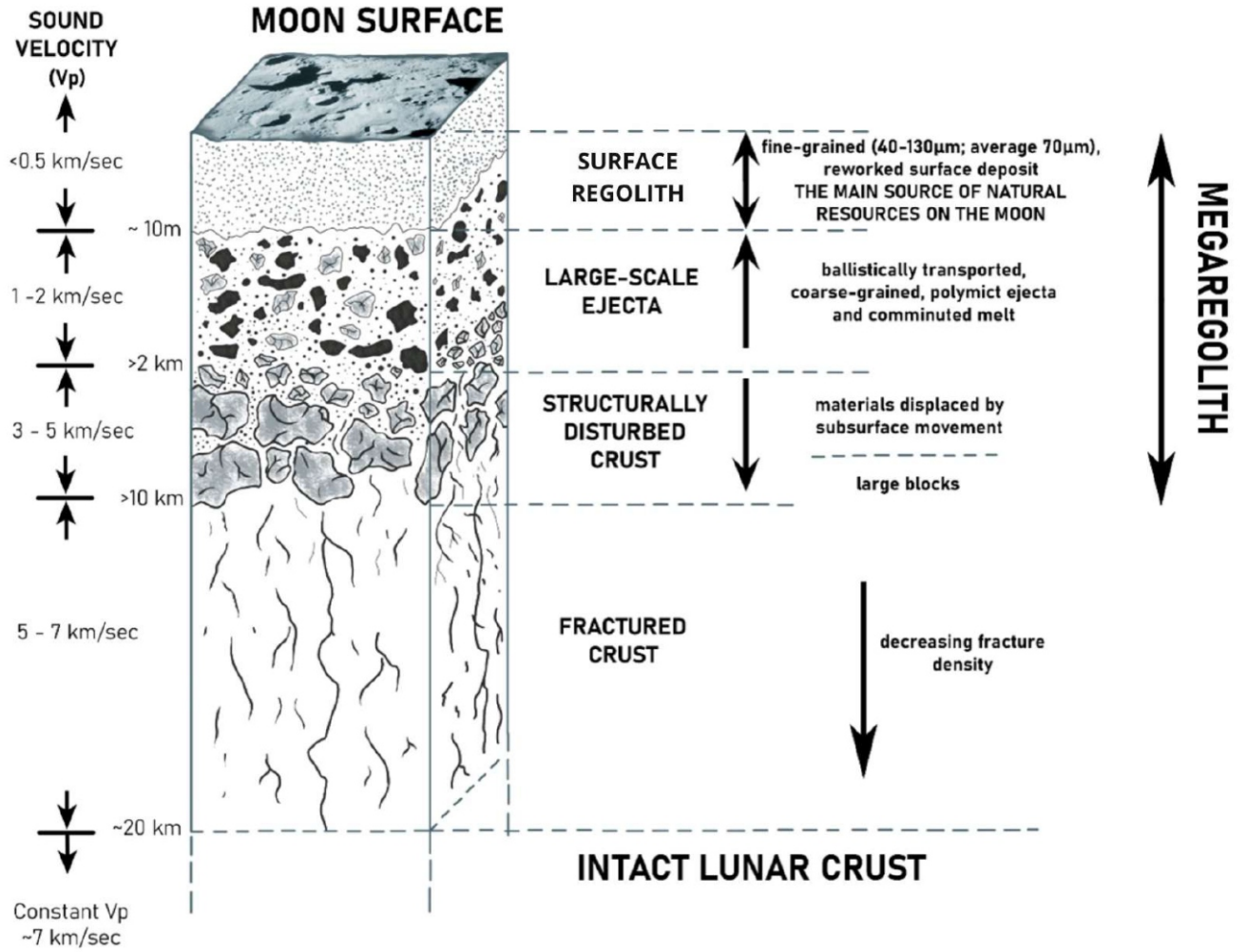

Fig. 1. Cross-section through the lunar regolith (figure by J. Przylibska, based on Jaumann et al., 2012)

bases as well. In addition, as in terrestrial conditions, fuel resources will be very important, to be used for rocket propulsion, as well as for the propulsion of devices, machines and robots working on the Moon, and as energy resources. The next group of raw materials that will always be needed are metals, as well as constructional raw materials (aggregates, rock raw materials, regolith, etc.). Finally, chemical raw materials will be needed for the chemical and materials industry (materials engineering).

THE AVERAGE CONTENT OF ELEMENTS IN LUNAR ROCKS

There is currently relatively good knowledge of the chemical element content of individual lunar rocks. In addition to studies of samples brought back by space missions, this knowledge is continually being expanded by studies of the chemical composition of lunar meteorites (Przylibski et al., 2023). Unlike samples brought back by lunar missions, samples delivered by meteorites can come from deeper as well as surface layers of the Moon.

Table 1 shows the average content of selected chemical elements in lunar rocks based on the results of chemical analyses of the composition of lunar meteorites. The elements characterized may be important in the context of their future extraction for use on the Moon (independent of the costly transport of raw materials from Earth). Full characterization of lunar rocks based on chemical analyses of meteorites is available in the Appendix 1 (Tables A1–A3). The data provided allow us to conclude that the average zinc and rhenium content is higher in anorthosites, while basalts and gabbros are significantly more enriched in scandium, titanium, vanadium, chromium, manganese, iron, germanium, REE, zirconium, niobium, hafnium, tantalum, thorium and uranium. This is due, among other things, to the main minerals composing these rocks: in the case of anorthosites, these are mainly plagioclases, to a lesser extent pyroxenes and olivines, while in the case of basalts, these are mainly pyroxenes and plagioclases, to a lesser extent olivines, ilmenite ($FeTiO_3$), and in small amounts also ulvöspinel (Fe_2TiO_4). Moreover, chlorapatite ($Ca_5(PO_4)_3Cl$) and zircon ($ZrSiO_4$) are also present in the KREEP basalts (Papike et al., 1991; Rubin, 1997; Rubin and Ma, 2017). The Appendix 1 (Table A4) also indicates the occurrence of minerals in the most important Moon rocks that contain important raw materials and can be considered ore-forming.

LIFE-SUSTAINING RAW MATERIALS – WATER AND OXYGEN

Among the raw materials that support the lives of humans, animals and plants, the most important is undoubtedly water, from which oxygen can also be obtained. Currently, it is widely believed that in the vicinity of the Moon's poles, in areas where sunlight does not reach (i.e. in permanently shadowed regions

Table 1

Characteristics of the most important lunar rocks in terms of the contents of selected chemical elements based on chemical analyses of rocks obtained from lunar meteorites (our results based on Koblitz, 2010)

Element	Unit	Anorthosite			Basalt			Gabbro		
		n	Arith. mean	Range	n	Arith. mean	Range	n	Arith. mean	Range
Al	%	82	14.707	11.02–18.50	12	6.846	4.287–8.700	7	6.038	5.27–7.11
Si	%	57	20.896	20.10–21.72	9	21.822	20.52–22.80	6	20.963	18.70–22.00
P	%	15	0.032	0.009–0.135	2	0.037	0.35–0.39	2	0.075	0.022–0.127
S	%	2	0.300	0.19–0.41	0	–	–	2	0.335	0.190–0.480
K	%	89	0.031	0.010–0.199	11	0.056	0.017–0.116	9	0.043	0.020–0.108
Sc	ppm	100	9.24	4.02–21.24	39	47.79	27.20–61.70	16	91.36	24.40–112.60
Ti	%	74	0.142	0.018–0.500	11	0.991	0.390–2.313	6	1.598	0.911–3.433
V	ppm	57	25.20	5.60–55.30	13	112.53	80.00–135.00	4	76.25	53.00–92.00
Cr	%	99	0.070	0.038–0.140	37	0.202	0.068–0.424	13	0.196	0.075–0.507
Mn	%	81	0.052	0.023–0.109	11	0.174	0.077–0.232	7	0.237	0.139–0.283
Fe	%	99	3.655	2.20–7.53	12	13.67	10.900–17.640	9	17.182	14.200–19.300
Co	%	101	0.002	0.001–0.009	33	0.004	0.003–0.005	16	0.003	0.002–0.008
Ni	%	101	0.016	0.005–0.037	16	0.013	0.002–0.034	9	0.005	0.001–0.020
Zn	ppm	39	25.50	4.84–361.00	7	10.03	2.20–30.50	7	5.29	1.35–17.00
Ge	ppm	10	0.48	0.20–0.78	5	0.15	0.03–0.24	2	3.05	2.20–3.90
Y	ppm	13	8.57	4.60–12.80	9	40.90	26.40–73.16	1	22.30	22.30
Zr	ppm	80	37.83	15.40–354.00	37	146.82	60.00–260.00	9	107.67	45.00–190.00
Nb	ppm	8	2.29	1.00–3.60	9	8.56	5.00–15.26	0	–	–
Ru	ppm	1	0.93	0.93	1	0.001	0.001	0	–	–
Rh	ppm	–	–	–	0	–	–	0	–	–
Pd	ppb	–	–	–	1	3.90	3.90	0	–	–
La	ppm	110	2.45	0.65–21.83	39	9.85	4.69–15.30	18	3.87	1.44–8.50
Ce	ppm	104	6.11	1.31–54.10	39	26.25	12.28–39.60	17	11.08	4.22–22.40
Pr	ppb	10	0.73	0.22–1.21	5	3.56	1.82–5.14	0	–	–
Nd	ppm	99	3.63	0.83–29.50	39	16.54	8.10–28.00	10	9.49	3.97–12.30
Sm	ppm	109	1.11	0.24–9.55	39	5.42	2.38–8.89	17	3.27	1.46–4.75
Eu	ppm	109	0.83	0.64–1.55	39	1.04	0.66–1.41	17	1.00	0.34–1.37
Gd	ppm	34	1.44	0.30–10.50	10	5.25	2.88–10.18	5	4.47	2.35–5.90
Tb	ppm	96	0.24	0.05–1.94	39	1.23	0.52–2.03	16	0.90	0.72–1.23
Dy	ppm	78	1.56	0.35–13.28	15	5.30	3.15–11.80	8	5.83	3.06–7.50
Ho	ppm	57	0.36	0.08–2.67	10	1.20	0.66–2.43	5	1.41	1.10–1.70
Er	ppm	17	0.93	0.23–1.53	8	3.69	1.87–6.73	1	2.17	2.17
Tm	ppm	23	0.19	0.03–1.41	6	0.45	0.23–0.90	3	0.63	0.42–0.77
Yb	ppm	106	0.95	0.21–7.50	39	4.46	1.92–7.40	17	3.75	2.28–5.08
Lu	ppm	105	0.14	0.03–1.02	39	0.63	0.28–1.03	17	0.56	0.36–0.82
Hf	ppm	100	0.84	0.17–7.15	39	3.90	1.70–6.42	16	2.62	2.06–3.35
Ta	ppm	82	0.12	0.04–0.99	39	0.52	0.19–0.80	16	0.36	0.22–0.50
Re	ppb	12	7.49	0.45–44.00	5	0.28	0.01–0.61	1	0.02	0.02
Os	ppb	13	98.47	0.01–560.00	5	3.62	0.00009–9.30	1	380.00	380.00
Ir	ppb	93	17.62	2.90–510.00	11	5.74	0.10–12.00	6	61.22	0.30–310.00
Pt	ppm	–	–	–	1	0.01	0.01	0	–	–
Th	ppm	97	0.38	0.06–4.28	39	1.44	0.51–2.39	16	0.56	0.31–1.31
U	ppm	92	0.12	0.03–1.18	38	0.38	0.17–0.67	10	0.14	0.09–0.28

(PSRs)), there is water in the form of H_2O ice at the bottoms of some craters (Anand et al., 2012; Casanova et al., 2020). The water ice content in these areas can be as high as 2% (Hayne et al., 2015). Water ice may also occur elsewhere on the Moon in regolith layers, where H_2O and OH^- molecules are produced by solar wind protons interacting with the oxygen-rich surfaces of fragmented rock grains produced by micrometeorite impacts on the lunar regolith (Jaumann et al., 2012). Studies of lunar soil samples brought back by the Chinese Chang'e 5 mission have shown that the solidified impact glass droplets contained in the regolith contain significant amounts of water molecules. It is currently estimated that 2.7 10^{14} kg of water may be stored in the surface layer of regolith in solidified droplets of impact glass (He et al., 2023). Studies carried out on the basis of in-situ spectral observations, as well as further work on the results obtained within the Chang'e 5 mission, show an average content of hydroxyl groups in this area at the level of 28.5 ppm (Liu et al., 2022) up to 170 ppm of water (Zhou et al., 2022). Experimental work is also being carried out using lunar regolith simulants to chemically reduce the regolith in order to obtain oxygen, metals, and water from it (Schwandt et al., 2012; Lomax et al., 2020; Sargeant et al., 2021). However, most of the processes involved in obtaining oxygen from lunar rocks are highly energy-consuming (Taylor and Carrier, 1993; Crawford, 2015). Additionally, a side effect of obtaining oxygen in the process of reducing regolith, or more precisely ilmenite, may be the extraction of metallic iron (Schlüter and Cowley, 2020) and titanium. Rutile (TiO_2) can also be a source of Ti, from which oxygen can also be recovered (Crawford et al., 2023). There is also evidence from interpretations of orbital neutron spectroscopy (Sinitsyn, 2014) and Stratospheric Observatory for Infrared Astronomy (SOFIA) data (Honniball et al., 2020) that hydrogen concentrations may exceed 100 ppm in some areas of the highlands – twice the amount measured in samples taken by probes (Crawford, 2015; Crawford et al., 2023).

FUELS AND ENERGY RESOURCES

In the absence of fossil fuels on the Moon, solar cells and nuclear energy are likely to play the most significant roles in the production of thermal and electrical energy.

For over 30 years, a prospective lunar resource has been the isotope of the noble gas helium – ^{3}He. This isotope is considered a flagship mineral resource, with its extraction anticipated to take place from lunar regolith. ^{3}He is an exceptionally efficient and clean nuclear fuel that can be utilized in nuclear fusion reactions (D-^{3}He) as a substitute for tritium. However, this technology is still far from industrial implementation. The prospect of extracting ^{3}He from lunar regolith, discussed since the 1980s (NASA, 1988), still remains a distant possibility, especially when compared to other mineral resources noted. Furthermore, the development of nuclear fusion-based energy systems on Earth remains a similarly remote prospect. The ^{3}He isotope, being a component of the solar wind, can be implanted into mineral crystals that constitute the surface layer of the regolith. Consequently, the highest concentrations of ^{3}He are associated with areas where the solar wind flux is strongest and where the regolith is mature. The maturity of regolith refers to its prolonged exposure to cosmic radiation, which, among other effects, leads to a decrease in its reflectivity. Helium-3 is most efficiently accumulated in ilmenite ($FeTiO_3$) crystals. Thus, its richest deposits are associated with accumulations of this mineral within the regolith. Such regions include the maria on the Moon's near side, which are rich in titanium (ilmenite), particularly the Procellarum KREEP Terrane. In this area, the concentration of ^{3}He in the regolith is estimated to reach up to 20 ppb (by mass; Johnson et al., 1999) or even higher, up to 24 ppb (Fa and Jin, 2007; Kim et al., 2019). The total reserves of ^{3}He are estimated at ~6.6 10^8 kg, with the majority (3.7 10^8 kg) located on the near side of the Moon, while the remaining 2.9 10^8 kg are found on the far side (Fa and Jin, 2007, 2010). According to data presented by Crawford (2015), Crawford et al. (2023), the average concentration of helium-3 in the regolith is ~4 ppb.

One of the proposed methods for extracting ^{3}He from ilmenite in lunar regolith involves rapidly heating ilmenite crystals to a temperature of 1000 K, at which ~75% of the accumulated helium-3 is released from the crystal structure within 1 second (Song et al., 2021).

In addition to ^{3}He accumulations in regolith ilmenite, a fuel source for modern nuclear power plants based on nuclear fission is uranium (^{235}U). Elevated concentrations of uranium are associated with KREEP rocks, which are also enriched in thorium (Yamashita et al., 2010; Li et al., 2022a), likely due to the increased presence of phosphates and zircon crystals in these lunar rocks.

The production of H_2 and O_2 as rocket fuel is also critical, along with the extraction of elements essential for metallurgical and chemical processes (Anand et al., 2012; Schwandt et al., 2012; Bennett et al., 2020; Lomax et al., 2020; Casanova et al., 2020; Schlüter and Cowley, 2020; Rasera et al., 2020; Reiss et al., 2020). Hydrogen is significant not only as rocket fuel but also as a reducing agent in certain reactions for extracting oxygen and metals from their oxides (Crawford, 2015). The issue of hydrogen and oxygen availability on the Moon is discussed in the section on life-supporting resources.

METALS

Metals are essential for the production of machinery, equipment, and structural components for lunar buildings, vehicles, and rockets. They will also be used to manufacture various machines and devices that enable human habitation, research, and exploration of the Moon, as well as the preparation and execution of space missions to more distant celestial bodies in the Solar System (e.g., Mars) or beyond its boundaries.

From the perspective of potential mining activities on the Moon, accumulations of resources such as ilmenite ($FeTiO_3$) appear particularly intriguing. Ilmenite, along with plagioclases (mainly anorthite), pyroxenes, and olivines, is among the most abundant minerals in lunar rocks (Rubin and Ma, 2017; Rasera et al., 2020). Compared to asteroids (Ti <0.07% by weight), the Moon is significantly richer in titanium (5–8% by weight; lithophilic; Crawford, 2015) and may represent the best source of this metal beyond Earth. Ilmenite is an ore mineral for both titanium and iron, and it can constitute >25% by volume of titanium-rich basalts (Papike et al., 1998, as cited in Crawford, 2015). Other minerals found in lunar rocks can also serve as sources of metals. Of particular interest is zircon, a component of KREEP rocks, which is a potential source of zirconium, hafnium, and rare earth elements (REEs), as well as chromite ($FeCr_2O_4$), which provides chromium and iron.

Additionally, lunar rocks have been found to contain minerals such as armalcolite [$(Mg,Fe)Ti_2O_5$], rutile (TiO_2), zirconolite [$(Ca,Fe)][(Zr,REE)][(Ti,Nb)_2O_7$], chalcopyrite ($CuFeS_2$), cubanite ($CuFe_2S_3$), pentlandite [$(Ni,Fe)_9S_8$], and sphalerite (ZnS), although these minerals occur very rarely (Papike et al., 1991; Rubin, 1997; Rubin and Ma, 2017).

Plagioclases (anorthite) in anorthosites are significantly enriched in europium (Taylor and McLennan, 2010). The total REE content in the rocks of the Procellarum KREEP Terrane (PKT) is estimated to be ~1200 ppm (0.12 wt.%), with individual element concentrations varying widely from 3–5 ppm for europium or lutetium to 300 ppm for yttrium or cerium (Crawford, 2015).

Iron remains the primary metal used in the global economy. On the Moon, this metal, present in silicate forms (pyroxenes and olivines) and as an oxide (FeO), is abundant in all basalts,

particularly in KREEP rocks (Yamashita et al., 2010; Li et al., 2022a). The content of metallic iron in the regolith is ~0.5% by weight (Morris, 1980). This iron originates from three sources: meteoritic iron, iron released from disaggregated bedrock, and iron produced during the reduction of iron oxides in the regolith by solar wind-derived hydrogen (nano-phase Fe; Morris, 1980; see Crawford, 2015). The latter form of iron, due to its small size and occurrence within agglutinates, is challenging to extract. The remaining two forms of metallic iron constitute for 0.34 ±0.11 wt.% (Morris, 1980; see Crawford, 2015).

Assuming that ~2% of the regolith's volume consists of meteoritic material (Melosh, 2011; Jaumann et al., 2012), a significant portion of this material comprises of FeNi(Co) grains. For iron meteorites, this composition is nearly 100%, whereas for some carbonaceous chondrites, it is practically 0%. Assuming an average weight percentage of FeNi grains (in the form of kamacite, taenite, and, to a lesser extent, tetrataenite) in meteoritic material at ~80% (a mass ratio analogous to Earth's), and an average density of meteoritic regolith of 3.5 g/cm^3, it is estimated that ~3.64% of the regolith's mass consists of grains composed of Fe, Ni, and, to a lesser extent, Co, with minor inclusions of other metals. Thus, lunar regolith already constitutes a pre-fragmented polymetallic ore of iron, nickel, and cobalt.

Recently, the presence of hematite has also been identified on the Moon. This mineral (Fe_2O_3), which contains oxidized iron – Fe^{3+} – can form under the highly reducing conditions of the lunar surface due to the delivery of oxygen from the upper layers of Earth's atmosphere, facilitated by the influence of Earth's magnetic field. Hematite has been detected at high lunar latitudes and is more prevalent on the near side than on the far side (Li et al., 2020). On Earth, hematite is a widely exploited iron ore, however, the occurrence and potential accumulations (reserves) of hematite on the Moon undoubtedly require further investigation.

Another potentially important metal is aluminum, whose content in the regolith of the lunar highlands typically ranges from 10–18 wt.% (Keszthelyi, 2022). However, extracting aluminum will require breaking down the structure of plagioclase-anorthite ($Ca[Al_2Si_2O_8]$). Processes for recovering aluminum from this aluminosilicate are being developed, but most of these methods are highly energy-consuming (Taylor and Carrier, 1993; Duke et al., 2006; Landis, 2007; Schwandt et al., 2012).

Silicon constitutes 20% by weight of lunar rocks (Kayama et al., 2018; see also Table 1). It is essential for applications such as the production of systems that convert solar radiation into energy. Proposed methods for extracting this element are similar to those for aluminum (Taylor and Carrier, 1993; Duke et al., 2006; Landis, 2007; Schwandt et al., 2012). A significant challenge will likely be meeting the purity standards required for semiconductors, which silicon produced on the Moon will need to satisfy (Crawford, 2015; Crawford et al., 2023).

ROCK RESOURCES, CONSTRUCTION MATERIALS AND AGGREGATES

Rock materials, building resources, and aggregates will likely be useful for constructing lunar bases and human settlements, as well as associated industrial facilities, including for agriculture and mining.

To enable future extraction and processing of lunar resource deposits, suitable exploitation and processing technologies are already being developed (Just et al., 2020; Rasera et al., 2020; Reiss et al., 2020; Zwierzyński et al., 2021; Wasilewski, 2021; Li et al., 2022b). Additionally, consideration is being given to technologies and techniques for processing (e.g., sintering) and utilizing lunar regolith as a construction material or as a feedstock for 3D printing (Lim and Anand, 2019; Grossman et al., 2019). Understanding the physical properties and chemical composition of regolith is currently of great importance for the development of lunar mining, geotechnical engineering, and construction (Wasilewski et al., 2021; Wiśniewski et al., 2022). Given these applications of regolith, there is an urgent need to produce simulants (analogues) of lunar regolith (Pitcher et al., 2016; Dominguez and Whitlow, 2019). These simulants are essential for testing equipment intended for lunar missions, particularly rovers and devices designed for soil (regolith) sampling.

Rock material remaining as waste after the recovery of metals (Fe, Ni, Co, Ti, Cr, Al, Zr, Hf, Eu, and other REEs), fuels (H_2, O_2, ^3He), water (H_2O molecules and OH^- ions), and other resources could be utilized as aggregate or other construction materials. The waste material (gangue) remaining after the extraction of resources from regolith will still possess thermal insulation properties, making it suitable for covering lunar structures such as habitations, laboratories, agricultural facilities, and industrial buildings. Moreover, layers of such post-regolith waste would effectively shield against cosmic radiation and solar wind particles while also providing protection from impacts by micrometeorites and small meteorites. Additionally, rock fragments present on the lunar surface and in outcrops could serve as a source of rock materials essential for construction purposes.

CHEMICAL RESOURCES

KREEP rocks are enriched in potassium and phosphorus (Yamashita et al., 2010; Li et al., 2022a), which are important resources for the chemical industry. In these rocks, chlorine and phosphorus are sourced from chlorapatite $Ca_5(PO_4)_3Cl$ (Papike et al., 1991; Rubin, 1997; Rubin and Ma, 2017). Another significant element for chemical industry needs is sulphur, with lunar rocks containing 715 ±216 ppm (Fegley and Swindle, 1993). On the Moon, sulphur occurs in combination with iron as a simple sulphide – troilite (FeS). The source of troilite in lunar regolith is meteoritic material (Papike et al., 1991; Rubin, 1997; Rubin and Ma, 2017).

DISCUSSION

The extraction of resources on the Moon for lunar missions and bases is crucial for their success and sustained operation, especially when considering the high costs of transporting and safely landing supplies from Earth. For example, DHL, in partnership with Astrobotic, currently offers such a service at a cost of $1.2 million per kilogram (https://www.astrobotic.com/dhl-and-airbus-defence-and-space-support-astrobotic-to-develop-lunar-delivery-service/, accessed: March 22, 2024). While transportation costs are expected to decrease as demand for shipping goods between Earth and the Moon grows, they are unlikely to fall to a level that would make transporting essential materials cheaper than developing and implementing technologies to utilize locally available resources. This is particularly true for readily accessible resources that occur in high concentrations (with substantial reserves). In the context of the Moon's resource availability, practically every rock and mineral becomes a potential source of raw materials. A prime example of this is lunar regolith and its constituent minerals, from which water can be extracted something that would not even be considered in the case of terrestrial regolith, such as weathered rock. Similarly, the potential exists

to supply metals, fuels, energy carriers, as well as chemical and construction materials. Transporting these resources from Earth is, and will likely long remain, if not indefinitely, economically unviable.

The loose regolith layer is practically the only environment on the Moon where significant geochemical processes occur, leading to the formation of accumulations deposits of various mineral resources. And, at least on the lunar surface, there are no traces of magmatic, metamorphic, hydrothermal or tectonic activity of the lunar interior that could be responsible for processes leading to variations in the chemical composition of the inner layers of the Moon, which could lead to deposit formation. Due to the continuous overturning ("gardening") and mixing of regolith caused by meteorite impacts on the lunar surface, it is assumed that volatiles implanted by the solar wind are present not only on the surface of the regolith layer but also at deeper levels (Crawford, 2015). Analyses of cores collected during the Apollo missions have confirmed that the concentrations of these elements and chemical substances remain approximately constant within the near-surface regolith layer, which is 2–3 m thick (Fegley and Swindle, 1993, as cited in Crawford, 2015).

As demonstrated by the characteristics of occurrence and the proposed methods for extracting various mineral resources from regolith deposits, the most cost-effective technologies and techniques for both exploitation and processing should, and likely will, incorporate the simultaneous recovery of multiple resources. Different resources present in regolith deposits are expected to be extracted within a single technological workflow, employing several processes to recover multiple resources simultaneously. Examples of such resources include water, which can be utilized to produce both water itself and rocket fuels in the form of H_2 and O_2. The exploitation and processing of ilmenite could yield ^3He, implanted into its structure by the solar wind, as well as titanium (and potentially iron), which form part of ilmenite's composition and are valuable metallic resources. Additionally, oxygen, essential for respiration and chemical processes, can be derived from the same operation. Sulphur extraction could be combined with the recovery of other volatile elements. Furthermore, after specific mineral resources are extracted from the regolith deposit, the remaining "waste" will consist of regolith depleted in the exploited resources, effectively a gangue composed primarily of silicate minerals, silicate rock fragments, and glass. This residual material will remain a valuable resource, suitable for use as an insulating material, construction aggregate, or as raw material for 3D printing. This approach enables the design of regolith exploitation as an almost zero-waste process. Therefore, there is no doubt that regolith deposits should be regarded as multi-resource deposits.

The discussion clearly demonstrates that multi-resource regolith deposits should be sought in regions where the regolith layer is the thickest. Additionally, regolith accumulations enriched in components derived from cosmic erosion and space weathering of KREEP rocks will contain the highest concentrations of useful mineral constituents. This indicates that the near side of the Moon, particularly the basaltic mare regions, holds the greatest potential for a diverse range of resources. In the lunar highlands, significant accumulations are formed by feldspathic resources (anorthite), from which Al, Si, O, and Eu can be extracted. The oxygen content in anorthositic highland rocks exceeds 40% by weight, meaning that a regolith layer 5–20 m thick, with a density of ~2,000 kg/m^3, contains 4–16 metric tons of oxygen per square metre of surface area (Keszthelyi, 2022). However, the processes for extracting these components from silicate minerals are extremely energy-consuming and, therefore, very costly. The recovery of these resources will likely require the development of new methods for their exploitation and processing.

The available sources of the most important resources on the Moon are summarized in Table 2. The average content of selected resources in the regolith was calculated based on chemical analyses of lunar meteorites (anorthosites and basalts), chemical analyses of basalts collected during the Apollo missions (categorized by titanium content), and the average chemical composition of meteorites found within the regolith. Based on these calculations, it was assumed that anorthosites account for 88.91% of the mass (with an assumed density of 1.5 g/cm^3 and an average thickness of 12.5 m), basalts make up 6.54% of the mass (46% low-Ti basalts, 29% medium-Ti basalts, and 24% high-Ti basalts; assumed density of 1.5 g/cm^3 and average thickness of 4.5 m), and meteoritic regolith material constitutes 4.55% of the mass (assumed to represent 2% of the total regolith volume, with a density of 3.5 g/cm^3 and an average chemical composition based on the terrestrial mass distribution of meteorite types).

To calculate the total mass of the lunar regolith, the Moon's radius R was assumed to be 1,737 km. Using the formula for the surface area of a sphere $P = 4\ R^2$, the surface area was calculated as 37,895,643 km^2. Assuming an ideal spherical shape for the Moon, the volume of the regolith layer was estimated at 421,606 km^3, resulting in a total mass of 6.49 10^{17} kg (6.49 10^{14} tons). This assumption provides a reasonable approximation of the actual volume of the regolith. However, it may lead to an overestimation of the resource reserves created by reactions with the solar wind (^3He, H_2, OH^-, H_2O), which are predominantly concentrated in the near-surface layer, ~3 m thick.

Life-supporting resource deposits, such as water and oxygen, on the Moon are associated with regolith located in permanently shadowed craters in the polar regions. Therefore, regolith in these areas can be exploited to extract oxygen and water. Additionally, the processes used for oxygen extraction will likely facilitate the recovery of metals, primarily Fe, Ti, Ni and Co.

The most resource-rich regions on the Moon, containing regolith enriched with the greatest variety of materials, are the Procellarum KREEP Terrane in the west and Mare Tranquillitatis in the east. In these areas, the regolith hosts deposits of ilmenite $FeTiO_3$ – a source of Ti, Fe and O – as well as water, rare earth elements, Ni, Co and Cr. These metals originate from native lunar minerals such as chromite – $FeCr_2O_4$ and zircon – $ZrSiO_4$, as well as meteoritic (asteroidal) minerals, including kamacite, taenite, and tetrataenite – polymorphic forms of FeNi(Co). Chemical resources such as K, P, Cl, and S, along with energy resources like ^3He, U, and Th, are also present. Phosphorus and chlorine are derived from chlorapatite $Ca_5(PO_4)_3Cl$ and apatite (a group of arsenates, phosphates, and vanadates), which are also sources of uranium and thorium. These radioactive elements are additionally found in zircon crystals. Sulphur is sourced from meteoritic troilite (FeS), and potassium comes from potassium feldspar ($KAlSi_3O_8$). After the recovery of these resources, the residual material can serve as an excellent raw material for construction. It is estimated that a 5–20 m regolith layer in equatorial regions may contain 30 to 100 billion tons of water-equivalent solar-wind hydrogen (Keszthelyi, 2022). High-Ti mare basalts of the Mare Tranquillitatis and Oceanus Procellarum, covering ~2 million km^2, locally show ^3He concentrations in the regolith exceeding 20 ppb (Fa and Jin, 2007). Assuming a regolith thickness of 3 metres, the total ^3He mass for these two regions is estimated at 2 10^8 kg (Crawford, 2015). The ^3He concentration in regolith varies between 2.4 and 26 ppb (Schmitt, 2006). Studies have identified eight regions with higher ^3He concentrations, reaching up to ~25 ppb (Wagner et al., 2014; Kim et al., 2019). All these regions are small, with diameters <50 km, one of which is Mare Moscoviensis (Elvis et al., 2021).

Table 2

Estimated content and reserves of selected resources in lunar regolith

Raw material	Main sources	Estimated content in regolith	Estimated resources in regolith	Comment
O_2	Ice (H_2O) Anorthite ($Ca[Al_2Si_2O_8]$) Rutile (TiO_2) ilmenite ($FeTiO_3$)	40.000%	2.60×10^{17} kg	1
Si	Anorthite ($Ca[Al_2Si_2O_8]$)	20.013%	1.30×10^{17} kg	1
Al	Anorthite ($Ca[Al_2Si_2O_8]$)	13.429%	8.72×10^{16} kg	1
Fe	Ilmenite ($FeTiO_3$) Chromite ($FeCr_2O_4$) Kamacite (α-(FeNi)) Taenite (γ-(FeNi))	7.903%	5.13×10^{16} kg	1
Ni	Kamacite (α-(FeNi)) Taenite (γ-(FeNi))	0.379%	2.46×10^{15} kg	1
Ti	Ilmenite ($FeTiO_3$) Ulvöspinel ($TiFe_2O_4$)	0.334%	2.17×10^{15} kg	1
S	Troilite (FeS)	0.287%	1.86×10^{15} kg	1
Cr	Chromite ($FeCr_2O_4$)	0.078%	5.09×10^{14} kg	1
P	Chlorapatite ($Ca_5(PO_4)_3Cl$) Merrillite $Ca_9NaMg(PO_4)_7$	0.042%	2.71×10^{14} kg	1
H_2O	Ice (H_2O)	0.042%	2.70×10^{14} kg	4
K	Orthoclase ($K[AlSi_3O_8]$)	0.033%	2.12×10^{14} kg	1
Co	Kamacite (α-(FeNi)) Taenite (γ-(FeNi))	0.022%	1.42×10^{14} kg	1
Zr	Zirconium ($ZrSiO_4$)	43.276 ppm	2.81×10^{13} kg	1
REE	Zirconium ($ZrSiO_4$) Merrillite $Ca_9NaMg(PO_4)_7$ Apatite ($Ca_5(PO_4)_3$ (F,Cl,OH))	35.615 ppm	2.31×10^{13} kg	1
PGM (Platinum Group Metals)	Minerals found in meteorites	2.088 ppm	1.36×10^{12} kg	1
Th	Zirconium ($ZrSiO_4$)	0.432 ppm	2.81×10^{11} kg	1
			6.90×10^{11} kg	3
U	Zirconium ($ZrSiO_4$)	0.132 ppm	8.55×10^{10} kg	1
			1.77×10^{11} kg	3
^3He	Ilmenite ($FeTiO_3$) ^3He incorporated by solar wind into crystal structure	3 ppb	1.95×10^{9} kg	1
			1.70×10^{9} kg	5
			6.60×10^{8} kg	2

1 – authors' estimations, 2 – Fa and Jin (2007, 2010), 3 – Bruhaug and Phillips (2021), 4 – He et al. (2023), 5 – Crawford et al. (2023)

The ^3He concentration indicates that extracting 1 kg of ^3He would require processing 100 000 to 1 000 000 metric tons of regolith (Schmitt, 2020, cited in Keszthelyi, 2022), presenting a significant technological challenge. Metallic iron content in regolith is ~0.3% by weight (Crawford, 2015), meaning 5 kg of Fe can be obtained from 1 m^3 of regolith (Crawford, 2015). Additionally, 1 m^3 of regolith could potentially contain 300 g of Ni and 0.5 g of platinum group metals (PGMs) (Crawford, 2015).

The regolith in highland areas, composed primarily of anorthosites, is enriched mainly in Al, Si, O, and H, as well as Eu, and likely also in Fe, Ni, Co, and S of meteoritic origin.

The richest multi-resource deposits are expected in areas covered by the thickest regolith layers, particularly within the Procellarum KREEP Terrane. A map showing the most prospectively resource-rich areas on the lunar surface, based on the analysis of source materials and their discussion, is shown by the authors in Figure 2.

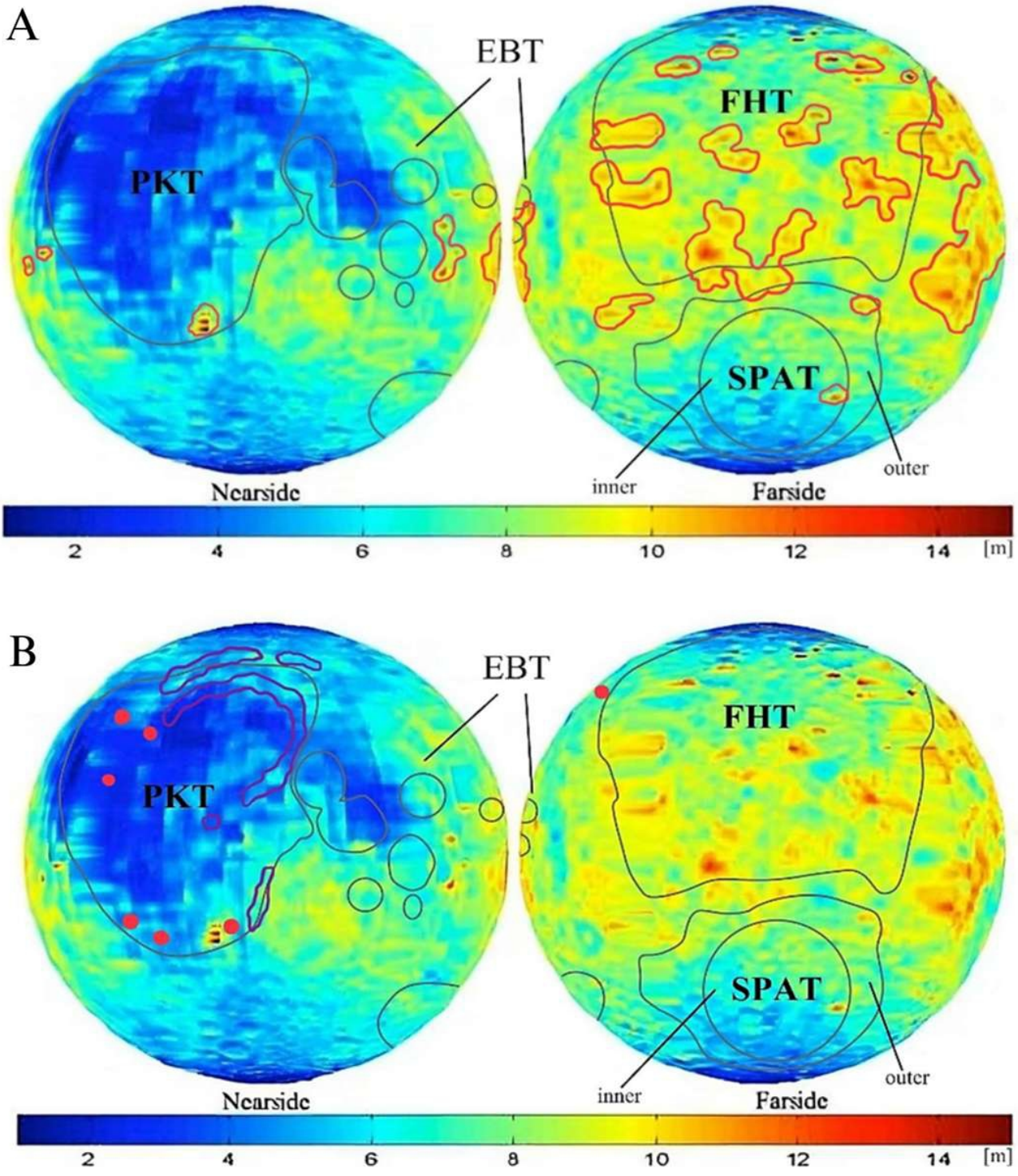

Fig. 2A – prospective areas for regolith deposits (see Table 2) identified based on the regolith thickness map (according to Fa and Jin, 2010) overlaid on lunar terrane boundaries (according to Jaumann et al., 2012); B – prospective areas for deposits associated with Mg-suite rocks (purple area) and silicic domes (red dots; according to Ji et al., 2022) overlaid on lunar terrane boundaries (according to Jaumann et al., 2012) and a regolith thickness map (according to Fa and Jin, 2010)

On the lunar surface, occurrences of felsic igneous rocks (rich in SiO_2) have been identified, forming domes that are either intrusions or extrusions (lava flows; Ji et al., 2022). These rocks may represent granites 4.4–3.9 Ga old, formed during at least eight magmatic pulses. They exhibit anhydrous mineral associations, significant enrichment in K/Ca, and low REE contents compared to KREEP rocks (Bonin, 2012). Due to their formation through several cycles of melting and crystallization, these rocks may serve as sources of accumulations of various incompatible elements, typically concentrated in residual melts. These could include various metals and chemical resources present in native forms, as oxides, sulphides, or salts of oxygenated and non-oxygenated acids. Such rocks, including pegmatites, as pneumatolytic and hydrothermal veins and pockets, may also be sources of silica in the form of quartz or other polymorphic variants of SiO_2. In regions such as the northern part of Oceanus Procellarum (Chang'e 5), these rocks could be enriched with precious metals, heavy metals, REEs,

Table 3

Potential raw material areas on the Moon

Area	Location on the Moon	Raw material-bearing rocks	Raw material
Maria	Basaltic maria (nearside)	regolith	^{3}He, Fe, Ti, K
		high-Ti basalts	Fe, Ti,
		breccias	Fe, Ti, Cr
	Procellarum KREEP Terrane	regolith	^{3}He, U, Th, Ti, Zr, Cr, REE, K, P
		KREEP rocks	U, Th, Fe, Ti, Zr, Cr, REE, K, P
	Mare Tranquillitatis	high-Ti basalts	Ti, K
	around Mare Imbrium	Mg-suite rocks	Cr, Mg
Highlands	South Pole Aitken Terrane	regolith, KREEP rocks	U, Th, K, P
	Lunar highlands	Anorthosites	Fe, Cr, Si, Al, O_2
Both maria and highlands	Silicic domes	silicic domes	Si
	North and south poles (PSR)	Ice	H_2O, O_2
	H/M Moon	Meteoritic material in regolith	PGM, Fe, Ni, S, Co

radioactive elements, and volatiles (e.g., F, B). They might also contain hydrated minerals and others such as muscovite, beryl, tourmaline, topaz, or lithium-bearing minerals. If pegmatitic rocks formed, they could potentially host ore-grade concentrations of some of these elements. However, these remain speculative, based on geochemical analogies with Earth and the shared genesis of Earth and the Moon (Zhang et al., 2022).

The lunar crust also comprises deep-seated igneous rocks of the magnesian suite (Mg-suite), including troctolites, spinel troctolites, norites, gabbronorites, and dunites. These rocks are found on the near side of the Moon and are spatially associated with KREEP rocks. These formations may hold potential for hosting deposits of metals commonly associated with mafic and ultramafic igneous rocks, such as Cr and platinum group metals (PGMs), similar to analogous deposits on Earth.

After thoroughly exploring regolith deposits, which should be easier and more cost-effective to exploit due to their multi-resource nature and pre-fragmented mineral components, the next step should involve investigating magmatic deposits in felsic rocks as well as in mafic and ultramafic rocks on the Moon.

At the current stage of lunar resource research, it is possible to make preliminary and very rough estimates of the reserves of some of the resources characterized. At present, only regolith deposits can be assessed for their resource potential. These are multi-resource deposits. On a global lunar scale, it is possible to estimate the reserves of individual resources contained in the regolith, particularly within its surface layer. The results of these estimates are shown in Table 2, while areas containing potential deposits are summarized in Table 3.

During the extraction, processing, and enrichment of resources from the regolith in the Procellarum KREEP Terrane, it will be crucial to separate ilmenite, zircon, chromite, and other mineral phases containing Fe, Ti, Cr, REE, U, Th, O, K, P, Cl, Ni, Co, and S from each other and from the gangue. Additionally, it will be necessary to isolate oxides, sulphides, silicates, phosphates, and native minerals such as FeNi(Co) separately from the ore. Density-based separation methods may yield satisfactory results for only some of the minerals. A significant advantage is the extremely fine grain size of the regolith, allowing many mineral components to exist as individual grains. However, at such fine sizes (40–130 μm), electrostatic interactions between grains begin to emerge, which will likely complicate the separation process. These are just a few examples of the challenges faced by engineers designing processing techniques and technologies for lunar regolith ore.

CONCLUSIONS

The Moon will serve as a source of raw materials necessary for constructing facilities and devices on its surface, as well as for generating energy and providing essential resources for human sustenance. Due to the high costs of transporting raw materials and supplies from Earth, any large-scale activities on the Moon require the utilization of resources extracted and processed near the sites of their use. Achieving independence from Earth-based resource deliveries is fundamental to the economic viability of maintaining a permanent human presence on the Moon.

The Moon's mineral resources are predominantly found within the regolith layer. This is because the regolith represents the only geochemically evolving layer of Earth's natural satellite over the past billion years. Lunar regolith should be considered as a multi-resource, pre-fragmented ore containing local enrichments of life-supporting, metallic, chemical, energy, and construction raw materials. Therefore, the primary focus of extraction and processing on the Moon will be regolith.

In addition to regolith, other potential resource zones include areas where outcrops or shallow subsurface deposits of mafic and ultramafic igneous rocks are present. These rocks may be enriched in metals such as Cr, Ti, REEs, and PGMs. Zones of felsic igneous rocks, enriched in quartz, also hold potential. These rocks may contain alkali elements and incompatible elements with silicate structures, such as precious metals, heavy metals, REEs, radioactive elements, and volatiles (e.g., F, B). They may also host hydrated minerals and components such as muscovite, beryl, tourmaline, topaz, or lithium-bearing minerals.

The most prospective areas for resource deposits are the lunar maria, which are potential sources of metals such as Fe, Ti, Cr, P, K, REEs, as well as energy resources like ^{3}He, U, and Th (Procellarum KREEP Terrane), while the polar regions, where water ice is present, are also crucial for human presence, as they provide a potential source of water, oxygen and hydrogen, making them fundamental for life support, energy, and enabling the operation of various industrial and agricultural processes. Outcrop zones of anorthosites on the Moon's far side, along with silica-rich rocks, could serve as sources of Si and Al, and the considerable volume and mass of meteoritic material in the regolith on both hemispheres of the Moon should also be taken into account, as this material already represents a pre-fragmented (enriched) source of metals such as Fe, Ni, Co, PGMs, and S.

Acknowledgements. The authors extend their gratitude to Jolanta Przylibska for creating Figure 1 and graphical abstract. The authors are also grateful to the reviewers, Professors Andrzej Muszyński and Zbigniew Sawłowicz, for their very constructive and favorable reviews. Thanks to these comments, our original manuscript undoubtedly gained in quality. We are also grateful to Professor Jan A. Zalasiewicz for linguistic correction.

REFERENCES

Anand, M., Crawford, I.A., Balat-Pichelin, M., Abanades, S., van Westrenen, W., Péraudeau, G., Jaumann, R., Seboldt, W., 2012. A brief review of chemical and mineralogical resources on the Moon and likely initial in situ resource utilization (ISRU) applications. Planetary and Space Science, **74**: 42–48; https://doi.org/10.1016/j.pss.2012.08.012

Barr, A.C., 2016. On the origin of Earth's Moon. Journal of Geophysical Research: Planets, **121**: 1573–1601; https://doi.org/10.1002/2016JE005098

Bennett, N.J., Ellender, D., Dempster, A.G., 2020. Commercial viability of lunar In-Situ Resource Utilization (ISRU). Planetary and Space Science, **182**; https://doi.org/10.1016/j.pss.2020.104842

Blutstein, K., 2021. Potential extraterrestrial sources of lithium. Geological Quarterly, **65**, 58; https://doi.org/10.7306/gq.1627

Bonin, B., 2012. Extra-terrestrial igneous granites and related rocks: A review of their occurrence and petrogenesis. Lithos, **153**: 3–24; https://doi.org/10.1016/j.lithos.2012.04.007

Borg, L.E., Gaffney, A.M., Shearer, C.K., 2015. A review of lunar chronology revealing a preponderance of 4.34–4.37 Ga ages. Meteoritics and Planetary Science, **50**: 715–732; https://doi.org/10.1111/maps.12373

Bruhaug, G., Phillips, W., 2021. Nuclear fuel resources of the moon: a broad analysis of future lunar nuclear fuel utilization. NSS Space Settlement Journal; https://nss.org/national-space-society-space-settlement-journal/

Carrier, D.W., Olhoeft, G.R., Mendell, W., 1991. Physical properties of the lunar surface. In: The Lunar Sourcebook: A User's Guide to the Moon (eds. G.H. Heiken, D. Vaniman and B.M. French): 475–594. Cambridge University Press, Cambridge.

Casanova, S., Espejel, C., Dempster, A.G., Anderson, R.C., Caprarelli, G., Saydam, S., 2020. Lunar polar water resource exploration – examination of the lunar cold trap reservoir system model and introduction of play-based exploration (PBE) techniques. Planetary and Space Science, **180**, 104742; https://doi.org/10.1016/j.pss.2019.104742

Crawford, I.A., 2015. Lunar resources: a review. Progress in Physical Geography, **39**: 137–167.

Crawford, I.A., Anand, M., Barber, S., Cowley, A., Crites, S., Fa, W., Flahaut, J., Gaddis, L., Greenhagen, B., Haruyama, J., Hurley, D., McLeod, C., Morse, A., Neal, C., Sargeant, H., Sefton-Nash, E., Tartese, R., 2023. Lunar Resources. Reviews in Mineralogy and Geochemistry, **89**: 829–868; https://doi.org/10.2138/rmg.2023.89.19

Dominguez, J.A., Whitlow, J., 2019. Upwards migration phenomenon on molten lunar regolith: New challenges and prospects for ISRU. Advances in Space Research, **63**: 2220–2228; https://doi.org/10.1016/j.asr.2018.12.014

Duke, M.B., Gaddis, L.R., Taylor, G.J., Schmitt, H.H., 2006. Development of the Moon. Reviews in Mineralogy and Geochemistry, **60**: 597–656; https://doi.org/0.1515/9781501509537-010

Elvis, M., Krolikowski, A., Milligan, T., 2021. Concentrated lunar resources: imminent implications for governance and justice. Philosophical Transactions of the Royal Society, A **379**, 20190563; https://doi.org/10.1098/rsta.2019.0563

Fa, W., 2020. Bulk Density of the Lunar Regolith at the Chang'E-3 Landing Site as Estimated From Lunar Penetrating Radar. Earth and Space Science, **7**, e2019EA000801; https://doi.org/10.1029/2019EA000801

Fa, W., Jin, Y.-Q., 2007. Quantitative estimation of helium-3 spatial distribution in the lunar regolith layer. Icarus, **190**: 15–23; https://doi.org/10.1016/j.icarus.2007.03.014

Fa, W., Jin, Y.-Q., 2010. Global inventory of Helium-3 in lunar regoliths estimated by a multi-channel microwave radiometer on the Chang-E 1 lunar satellite. Chinese Science Bulletin, **55**: 4005–4009; https://doi.org/10.1007/s11434-010-4198-9

Fegley, B., Swindle, T.D., 1993. Lunar volatiles: implications for lunar resource utilization. In: Resources of Near Earth Space (eds. J. Lewis, M.S. Matthews and M.L. Guerrieri): 367–426. Tucson University Press, Tucson.

Greeley, R., Batson, R., 1999. Atlas Układu Słonecznego NASA. Prószyński i S-ka, Warszawa.

Grossman, K.D., Sakthivel, T.S., Sibille, L., Mantovani, J.G., Seal, S., 2019. Regolith-derived ferrosilicon as a potential feedstock material for wire-based additive manufacturing. Advances in Space Research, **63**: 2212–2219; https://doi.org/10.1016/j.asr.2018.12.002

Gruszczyk, H., 1984. The science of deposits (in Polish). Wydaw. Geol., Warszawa.

Hadler, K., Martin, D.J.P., Carpenter, J., Cilliers, J.J., Morse, A., Starr, S., Rasera, J.N., Seweryn, K., Reiss, P., Meurisse, A., 2020. A universal framework for Space Resource Utilisation (SRU). Planetary and Space Science, **182**, 104811; https://doi.org/10.1016/j.pss.2019.104811

Hayne, P.O., Hendrix, A., Sefton-Nash, E., Siegler, M.A., Lucey, P.G., Retherford,, K.D., Williams J.-P., Greenhagen, B.T., Paige, D.A., 2015. Evidence for exposed water ice in the Moon's south polar regions from Lunar Reconnaissance Orbiter ultraviolet albedo and temperature measurements. Icarus, **255**: 58–69; https://doi.org/10.1016/j.icarus.2015.03.032

He, H., Ji, J., Zhang, Y., Hu, S., Lin, Y., Hui, H., Hao, J., Li, R., Yang, W., Tian, H., Zhang, Ch., Anand, M., Tartèse R., Gu L., Li J., Zhang D., Mao Q., Jia L., Li X., Chen Y., Zhang L., Ni H., Wu, S., Wang, H., Li, Q., He, H., Xianhua, Li X., Wu, F., 2023. A solar wind-derived water reservoir on the Moon hosted by impact glass beads. Nature Geoscience, **16**: 294–300; https://doi.org/10.1038/s41561-023-01159-6

Honniball, C.I., Lucey, P.G., Li, S., Shenoy, S., Orlando, T.M., Hibbitts, C.A., Hurley, D.M., Farrell, W.M., 2020. Molecular water detected on the sunlit Moon by SOFIA. Nature Astronomy Letters, **5**: 121–127; https://doi.org/10.1038/s41550-020-01222-x

Jaumann, R., Hiesinger, H., Anand, M., Crawford, I.A., Wagner, R., Sohl, F., Jolliff, B.L., Scholten, F., Knapmeyer, M., Hoffmann, H., Hussmann, H., Grott, M., Hempel, S., Köhler, U., Krohn, K., Schmitz, N., Carpenter, J., Wieczorek, M., Spohn, T., Robinson, M.S., Oberst, J., 2012. Geology, geochemistry, and geophysics of the Moon: Status of current understanding. Planetary and Space Science, **74**: 15–41; https://doi.org/10.1016/j.pss.2012.08.019

Ji, J., Guo, D., Liu, J., Chen, S., Ling, Z., Ding, X., Han, K., Chen, J., Cheng, W., Zhu, K., Liu, J., Wang, J., Chen, J., Ouyang, Z., 2022. The 1:2,500,000-scale geologic map of the global Moon. Science Bulletin, **67**, 15; https://doi.org/10.1016/j.scib.2022.05.021

Jin, Y.-Q., Fa, W., Wieczorek, M.A., 2010. Preliminary analysis of microwave brightness temperature of the lunar surface from Chang-E 1 multi-channel radiometer observation and inversion of regolith layer thickness. 41st Lunar and Planetary Science Conference, 1331.pdf

Johnson, J.R., Swindle, T.D., Lucey, P.G., 1999. Estimated Solar Wind-Implanted Helium-3 Distribution on the Moon. Geophysical Research Letters, **26**: 385–388; https://doi.org/10.1029/1998GL900305

Just, G.H., Smith, K., Joy, K.H., Roy, M.J., 2020. Parametric review of existing regolith excavation techniques for lunar In Situ Resource Utilisation (ISRU) and recommendations for future excavation experiments. Planetary and Space Science, **180**; https://doi.org/10.1016/j.pss.2019.104746

Kallio, E., Dyadechkin, S., Wurz, P., Khodachenko, M., 2019. Space weathering on the Moon: Farside-nearside solar wind precipitation asymmetry. Planetary and Space Science, **166**: 9–22; https://doi.org/10.1016/j.pss.2018.07.013

Kayama, M., Nagaoka, H., Niihara, T., 2018. Lunar and Martian Silica. Minerals, **8**, 267; https://doi.org/10.3390/min8070267

Keszthelyi, L.P., Coyan, J.A., Bennett, K.A., Ostrach, L.R., Gaddis, L.R., Gabriel, T.S., Hagerty, J., 2023. Assessment of lunar resource exploration in 2022 (No. 1507). US Geological Survey.

Kim, K.J., Wöhler, C., Berezhnoy, A.A., Bhatt, M., Grumpe, A., 2019. Prospective ^{3}He-rich landing sites on the Moon. Planetary Space Sciences, **177**, 104686; https://doi.org/10.1016/j.pss.2019.07.001

Koblitz, J., 2010. MetBase® ver. 7.3. Meteorite Data Retrival Software. Ritterhude, Germany.

Landis, G.A., 2007. Materials refining on the Moon. Acta Astronautica, **60**: 906–915.

Lawrence, D.J., Feldman, W.C., Prettyman, T.H., 2000. Thorium abundances on the lunar surface. Journal of Geophysical Research, **105**: 20,307–20,331; https://doi.org/10.1029/1999JE001177

Li, Ch., Hu, H., Yang, M., Pei, Z., Zhou, Q., Ren, X., Liu, B., Liu, D., Zeng, X., Zhang, G., Zhang, H., Liu, J., Wang, Q., Deng, X., Xiao, C., Yao, Y., Xue, D., Zuo, W., Su, Y., Wen, W., Ouyang, Z., 2022a. Characteristics of the lunar samples returned by the Chang'E-5 mission. National Science Review, **9**, nwab188; https://doi.org/10.1093/nsr/nwab188

Li, Ch., Wei, K., Li, Y., Ma, W., Lei, Y., Yu, H., Liu, J., 2022b. A novel strategy to extract lunar mare KREEP-rich metal resources using a silicon collector. Journal of Rare Earths, **41**: 1429–1436; https://doi.org/10.1016/j.jre.2022.07.002

Li, S., Lucey, P.G, Fraeman, A.A., Poppe, A.R., Sun, V.Z., Hurley, D.M., Schultz P.H., 2020. Widespread hematite at high latitudes of the Moon. Science Advances, **6**, 36; https://doi.org/10.1126/sciadv.aba1940

Lim, S., Anand, M., 2019. Numerical modelling of the microwave heating behaviour of lunar regolith. Planetary and Space Science, **179**, 104723; https://doi.org/10.1016/j.pss.2019.104723

Liu, J., Liu, B., Ren, X., Li, Ch., Shu, R., Guo, L., Yu, S., Zhou, Q., Liu, D., Zeng, X., Gao, X., Zhang, G., Yan, W., Zhang, H., Jia, L., Jin, S., Xu, Ch., Deng, X., Xie, J., Yang, J., Huang, Ch., Zuo, W., Su, Y., Wen, W., Ouyang, Z., 2022. Evidence of water on the lunar surface from Chang'E-5 in-situ spectra and returned samples. Nature Communications, **13**: 3119; https://doi.org/10.1038/s41467-022-30807-5

Lock, S.J., Stewart, S.T., Petaev, M.I., Leinhardt, Z., Mace, M.T., Jacobsen, S.B., Ćuk, M., 2018. The origin of the Moon within a terrestrial synestia. Journal of Geophysical Research: Planets, **123**: 910–951; https://doi.org/10.1002/2017JE005333

Lomax, B.A., Conti, M., Khan, N., Bennett, N.S., Ganin, A.Y., Symes, M.D., 2020. Proving the viability of an electrochemical process for the simultaneous extraction of oxygen and production of metal alloys from lunar regolith. Planetary and Space Science, **180**, 104748; https://doi.org/10.1016/j.pss.2019.104748

Łuszczek, K., Przylibski, T.A., 2019. Potential deposits of selected metallic resources on L chondrite parent bodies. Planetary and Space Science, **168**: 40–51; https://doi.org/10.1016/j.pss.2019.02.005

Łuszczek, K., Przylibski, T.A., 2021. Selected metal resources on H chondrite parent bodies. Planetary and Space Science, **206**, 105309; https://doi.org/10.1016/j.pss.2021.105309

Mayer, C., 2012. Lunar Sample Compendium. Astromaterials Research & Exploration Science (ARES), NASA; ttps://curator.jsc.nasa.gov/lunar/lsc/index.cfm; accessed: 26.01.2023.

McKay, D.S., Heiken, G., Basu, A., Blanford, G., Simon, S., Reedy, R., French, B.M., Papike, J., 1991. The lunar regolith. In: Lunar Sourcebook (eds. G.H. Heiken, D.T. Vaniman and B.M. French): 285–356. Cambridge University Press.

Melosh, H.J., 2011. Planetary Surface Processes. Cambridge University Press, Cambridge.

MetBull, 2023. The Meteoritical Bulletin Database, The Meteoritical Society; https://www.lpi.usra.edu/meteor/ ; dostęp: 16.05.2023.

Metzger, A.E., Parker, R.E., 1979. The distribution of titanium on the lunar surface. Earth and Planetary Science Letters, **45**: 155–171; https ://doi.org/10.1016/0012-821X(79)90117-1

Migaszewski, Z.M., Gałuszka, A., 2007. Basics of environmental geochemistry (in Polish). Wydaw. Naukowo-Techniczne, Warszawa.

Morris, R.V., 1980. Origins and size distribution of metallic iron particles in the lunar regolith. Proceedings of the Lunar and Planetary Science Conference, **11**: 1697–1712.

Mutch, T.A., 1972. Geology of the Moon: A Stratigraphic View. Princeton University Press; http://www.jstor.org/stable/j.ctt13x0w46

NASA, 1988. Lunar Helium-3 and Fusion Power. Proceedings of a workshop sponsored by the NASA Office of Exploration and the Department of Energy Office of Fusion Energy and held at the NASA Lewis Research Center Cleveland, Ohio April 25 and 26. National Aeronautics and Space Administration Scientific and Technical Information Branch.

Papike, J.J., Simon, S.B., Laul, J.C., 1982. The lunar regolith: Chemistry, mineralogy, and petrology. Reviews of Geophysics, **20**, 761; https://doi.org/10.1029/rg020i004p00761

Papike, J., Taylor, L., Simon, S., 1991. Lunar minerals. In: Lunar Sourcebook (eds. G.H. Heiken, D.T. Vaniman and B.M. French): 121–181. Cambridge University Press, Cambridge.

Papike, J.J., Ryder, G., Shearer, C.K., 1998. Lunar samples. Reviews in Mineralogy and Geochemistry, **36**: 5.1–5.234.

Pitcher C., Kömle N., Leibniz O., Morales-Calderon O., Gao Y., Richter L., 2016. Investigation of the properties of icy lunar polar regolith simulants. Advances in Space Research, **57**: 1197–1208; https://doi.org/10.1016/j.asr.2015.12.030

Polański, A., 1988. Basics of geochemistry (in Polish). Wydaw. Geol., Warszawa.

Przylibski, T.A., Łuszczek, K., Blutstein, K., Szczęśniewicz, M., Ciapka, D., 2022. Extraterrestrial mining in Poland (in Polish with English summary). Przegląd Górniczy, (3): 17–24.

Przylibski, T.A., Blutstein, K., Szczęśniewicz, M., Łuszczek, K., 2023. First Ton of Moon on Earth (in Polish with English summary). Acta Societatis Metheoriticae Polonorum, **14**: 163-182.

Przylibski, T.A., Szczęśniewicz, M., Blutstein, K., 2024. Are there natural analogues of Moon rocks in Lower Silesia? (in Polish with English summary). Przegląd Geologiczny, **72**: 26–46; https://doi.org/10.7306/2024.2

Qin, L., Yue, Z., Gou, S., Zhang, Y., Wei, G., Shi, K., Zhang, X., Yang, B., 2025. Structure and Formation Mechanism of Lunar Regolith. Space: Science & Technology, **5**, 0219; https://doi.org/10.34133/space.0219

Rasera, J.N., Cilliers, J.J., Lamamy, J.A., Hadler, K., 2020. The beneficiation of lunar regolith for space resource utilisation: a review. Planetary and Space Science, **186**, 104789; https://doi.org/10.1016/j.pss.2020.104879

Reiss, P., Kerscher, F., Grill, L., 2020. Thermogravimetric analysis of chemical reduction processes to produce oxygen from lunar regolith. Planetary and Space Science, **181**, 104795; https://doi.org/10.1016/j.pss.2019.104795

Rubin, A.E., 1997. Mineralogy of meteorite groups. Meteoritics & Planetary Science, **32**: 231–247; https://doi.org/10.1111/j.1945-5100.1997.tb01262.x

Rubin, A.E., Ma, C., 2017. Meteoritic minerals and their origins. Chemie der Erde, **77**: 325–385; https://doi.org/10.1016/j.chemer.2017.01.005

Sargeant, H.M., Barber, S.J., Anand, M., Abernethy, F.A.J., Sheridan, S., Wright, I.P., Morse, A.D., 2021. Hydrogen reduction of lunar samples in a static system for a water production demonstration on the Moon. Planetary and Space Science, **205**, 105287; https://doi.org/10.1016/j.pss.2021.105287

Schlüter, L., Cowley, A., 2020. Review of techniques for in-situ oxygen extraction on the Moon. Planetary and Space Science, **181**, 104753; https://doi.org/10.1016/j.pss.2019.104753

Schmitt, H.H., 2006. Return to the Moon – Exploration, Enterprise, and Energy in the human Settlement of Space. New York, Springer.

Schmitt, H.H., 2020. Lunar hydrogen and helium resource development, in ASCEND 2020 Meeting, virtual, November 16–18, 2020: American Institute for Aeronautics and Astronautics, paper 2020-4001; https://doi.org/10.2514/6.2020-4001

Schwandt, C., Hamilton, J.A., Fray, D.J., Crawford, I.A., 2012. The production of oxygen and metal from lunar regolith. Planetary and Space Science, **74**: 49–56; https://doi.org/10.101 6/j.pss.2012.06.011

Sinitsyn, M.P., 2014. The hydrogen anomalies in KREEP terrain according to the results of LEND and LPNS neutron spectrometer data. In: 2nd European Lunar Symposium, London, May 2014, 17–18; http://sservi.nasa.gov/wp-content/uploads/2014/05/ELS2014_ProgAbstractBook_07May.pdf; accessed: December 2014.

Smirnow, W.I., 1986. Geology of mineral deposits (in Polish). Wydaw. Geol., Warszawa.

Song, H., Zhang, J., Sun, Y., Li, Y., Zhang, X., Ma, D., Kou, J., 2021. Theoretical Study on Thermal Release of Helium-3 in Lunar Ilmenite. Minerals, **11**, 319; https://doi.org/10.3390/min11030319

Taylor, L.A., Carrier, W.D., 1993. Oxygen production on the Moon: an overview and evaluation. In: Resources of Near Earth Space (eds. J. Lewis, M.S. Matthews and M.L. Guerrieri): 69–108. Tucson University Press, Tucson.

Taylor, S.R., McLennan, S.M., 2010. Planetary crusts: their composition, origin and evolution. Cambridge University Press, Cambrige.

Wagner, R.V., Robinson, M.S., 2014. Distribution, formation mechanisms, and significance of lunar pits. Icarus, **237**: 52–60; https://doi.org/10.1016/j.icarus.2014.04.002

Wasilewski, T.G., 2021. Lunar thermal mining: Phase change interface movement, production decline and implications for systems engineering. Planetary and Space Science, **199**, 105199; https://doi.org/10.1016/j.pss.2021.105199

Wasilewski, T.G., Barciński, T., Marchewka, M., 2021. Experimental investigations of thermal properties of icy lunar regolith and their influence on phase change interface movement. Planetary and Space Science, **200**, 105197; https://doi.org/10.1016/j.pss.2021.105197

Williams, D.M., Zugger, M.E., 2024. Forming Massive Terrestrial Satellites through Binary-exchange Capture. The Planetary Science Journal, **5**, 208; https://doi.org/10.3847/PSJ/ad5a9a

Wiśniewski, Ł., Wasilewski, G., Kędziora, B., Grygorczuk, J., 2022. Wybrane właściwości regolitu i ich istotny wpływ na realizację misji eksploracyjnych (in Polish). Acta Societatis Metheoriticae Polonorum, **13**: 107–119.

Yamashita, N., Hasebe, N., Reedy, R.C., Koboyashi, S., Karouji, Y., Hareyama, M., Shibamura, E., Kobayashi, M.-N., Okudaira, O., d'Uston, C., Gasnault, O., Forni, O., Kim, K.J., 2010. Uranium on the Moon: Global distribution and U/Th ratio. Geophysical Research Letters, **37**, L10201; https://doi.org/10.1029/2010GL043061

Zhang, B., Lin, Y., Moser, D.E., Warren, P.H., Hao, J., Barker, I.R., Shieh, S.R., Bouvier, A., 2021. Timing of lunar Mg-suite magmatism constrained by SIMS U-Pb dating of Apollo norite 78238. Earth and Planetary Science Letters, **569**, 117046; https://doi.org/10.1016/j.epsl.2021.117046

Zhang, H., Zhang, X., Zhang, G., Dong, K., Deng, X., Gao, X., Yang, Y., Xiao, Y., Bai, X., Liang, K., Liu, Y., Ma, W., Zhao, S., Zhang, C., Zhang, X., Song, J., Yao, W., Chen, H., Wang, W., Zou, Z., Yang, M., 2022. Size, morphology, and composition of lunar samples returned by Chang'E-5 mission. Science China Physics, Mechanics & Astronomy, **65**, 229511; https://doi.org/10.1007/s11433-021-1818-1

Zhou, Ch., Tang, H., Li, X., Zeng, X., Mo, B., Yu, W., Wu, Y., Zeng, X., Liu, J., Wen, Y., 2022. Chang'E-5 samples reveal high water content in lunar minerals. Nature Communications, **13**, 5336; https://doi.org/10.1038/s41467-022-33095-1

Zhou, Y., Bi, R., Liu, Y., 2024. Research Advances in the Giant Impact Hypothesis of Moon Formation. Space: Science & Technology, **4**, 0153; https://doi.org/10.34133/space.0153

Zwierzyński, A.J., Teper, W., Wiśniowski, R., Gonet, A., Buratowski, T., Uhl, T., Seweryn, K., 2021. Feasibility study of low mass and low energy consumption drilling devices for future space (mining surveying) missions. Energies, **14**, 5005; https://doi.org/10.3390/en14165005

Author contributions

The research idea and concept of the article – TAP. Preparation of data for tables and their creation – KB and MS. Preparation of data for figures (except Fig. 1) and their creation – MS. Preparation of appendices – KB. Initial text editing – TAP. Development of results, discussion, and final text editing – all authors.

Conflict of interest

The authors declare that there are no conflicts of interest related to the publication of this article and that there are no financial ties to disclose.

Informed consent

Consent for publication has been obtained.

Funding

The work was entirely financed by the authors private funds.

APPENDIX 1

Table A1. Characteristics of lunar anorthosites in terms of the content of selected chemical elements based on chemical analyses of rocks obtained from lunar meteorites (authors' own work based on Koblitz, 2010)

	unit	n	mean	median	deviation	range
H	ppm	4	450	410	290	170–820
Li	ppm	5	2.88	2.90	0.24	2.49–3.20
Be	ppb	1	0.50	0.50	0	0.50
B	ppb	0	–	–	–	–
C	%	0	–	–	–	–
N	%	0	–	–	–	–
F	ppm	2	39	39	9	30–48
Na	%	90	0.269	0.250	0.059	1.61–6.10
Mg	%	80	3.098	3.030	0.773	1.45–5.30
Al	%	82	14.707	14.800	0.970	11.02–18.50
Si	%	57	20.896	21.00	0.319	20.10–21.72
P	%	15	0.032	0.025	0.032	0.009–0.135
S	%	2	0.30	0.30	0.11	0.19–0.41
Cl	ppm	8	155.88	82.50	149.94	10–382
K	%	89	0.031	0.024	0.023	0.010–0.199
Ca	%	90	11.565	11.620	0.704	9.51–14.20
Sc	ppm	100	9.24	8.47	2.87	4.02–21.24
Ti	%	74	0.142	0.140	0.060	0.018–0.500
V	ppm	57	25.20	24.00	9.09	5.60–55.30
Cr	%	99	0.070	0.064	0.018	0.038–0.140
Mn	%	81	0.052	0.051	0.012	0.023–0.109
Fe	%	99	3.655	3.390	0.834	2.20–7.53
Co	%	101	0.002	0.002	0.001	0.001–0.009
Ni	%	101	0.016	0.015	0.006	0.005–0.037
Cu	ppm	0	–	–	–	–
Zn	ppm	39	25.50	12.00	56.02	4.84–361.00
Ga	ppm	67	4.54	3.51	5.35	2.40–45.70
Ge	ppm	10	0.48	0.42	0.20	0.20–0.78
As	ppm	24	0.26	0.18	0.24	0.03–1.02
Se	ppm	13	0.33	0.30	0.13	0.16–0.60
Br	ppm	46	1.86	0.81	5.63	0.04–38.90
Rb	ppm	20	1.75	0.99	2.40	0.16–9.37
Sr	ppm	92	193.61	158.00	116.49	118–890
Y	ppm	13	8.57	9.19	2.90	4.60–12.80
Zr	ppm	80	37.83	33.00	37.38	15.40–354.00
Nb	ppm	8	2.29	2.50	0.88	1.00–3.60
Mo	ppm	5	1.31	1.20	0.41	0.87–1.80
Ru	ppm	1	0.93	0.93	0	0.93
Rh	ppm	–	–	–	–	–
Pd	ppb	–	–	–	–	–
Ag	ppb	5	12.08	7.02	10.03	3.40–30.00
Cd	ppb	13	33.02	14.80	48.48	6.30–190.00
In	ppb	4	4.57	3.34	3.32	1.60–10.00
Sn	ppm	7	0.36	0.24	0.22	0.11–0.71
Sb	ppb	26	36.70	32.00	32.73	2.00–151.00
Te	ppb	4	27.65	16.15	24.81	8.30–70.00
I	ppm	5	0.99	0.91	0.77	0.16–2.10
Cs	ppb	53	78.88	55.00	97.31	6.20–550.00
Ba	ppm	100	73.66	31.00	111.22	18.30–820.00
La	ppm	110	2.45	2.30	2.10	0.65–21.83
Ce	ppm	104	6.11	5.82	5.29	1.31–54.10
Pr	ppb	10	0.73	0.83	0.37	0.22–1.21
Nd	ppm	99	3.63	3.30	2.89	0.83–29.50
Sm	ppm	109	1.11	1.05	0.92	0.24–9.55
Eu	ppm	109	0.83	0.79	0.14	0.64–1.55
Gd	ppm	34	1.44	1.10	1.65	0.30–10.50
Tb	ppm	96	0.24	0.23	0.19	0.05–1.94
Dy	ppm	78	1.56	1.40	1.40	0.35–13.28
Ho	ppm	57	0.36	0.31	0.33	0.08–2.67
Er	ppm	17	0.93	0.85	0.40	0.23–1.53
Tm	ppm	23	0.19	0.13	0.26	0.03–1.41
Yb	ppm	106	0.95	0.88	0.71	0.21–7.50
Lu	ppm	105	0.14	0.13	0.10	0.03–1.02
Hf	ppm	100	0.84	0.80	0.71	0.17–7.15
Ta	ppm	82	0.12	0.10	0.11	0.04–0.99
W	ppm	12	0.41	0.25	0.50	0.08–2.00

Re	ppb	12	7.49	0.61	15.46	0.45–44.00
Os	ppb	13	98.47	0.01	195.71	0.01–560.00
Ir	ppb	93	17.62	6.10	71.38	2.90–510.00
Pt	ppm	–	–	–	–	–
Au	ppb	94	5.33	2.90	7.84	0.60–62.00
Hg	ppm	–	–	–	–	–
Tl	ppb	4	4.29	4.47	2.61	0.97–7.25
Pb	ppm	8	0.73	0.70	0.36	0.17–1.30
Bi	ppb	4	3.87	1.41	4.73	0.64–12.00
Th	ppm	97	0.38	0.34	0.44	0.06–4.28
U	ppm	92	0.12	0.10	0.13	0.03–1.18

Table A2. Characteristics of lunar basalts in terms of the content of selected chemical elements based on chemical analyses of rocks obtained from lunar meteorites (authors' own work based on Koblitz, 2010)

	unit	n	mean	median	deviation	range
H	ppm	0	–	–	–	–
Li	ppm	8	6.46	4.83	3.35	3.99–12.69
Be	ppb	8	0.93	0.91	0.26	0.60–1.37
B	ppb	0	–	–	–	–
C	%	0	–	–	–	–
N	%	0	–	–	–	–
F	ppm	0	–	–	–	–
Na	%	11	0.282	0.280	0.037	0.231–0.370
Mg	%	12	4.808	4.650	1.076	3.330–7.420
Al	%	12	6.846	6.980	1.319	4.287–8.700
Si	%	9	21.822	22.100	0.717	20.52–22.80
P	%	2	0.37	0.37	0.02	0.35–0.39
S	%	0	–	–	–	–
Cl	ppm	1	134.00	134.00	0	134.00
K	%	11	0.056	0.049	0.026	0.017–0.116
Ca	%	12	8.100	8.140	0.809	5.99–9.20
Sc	ppm	39	47.79	46.71	11.86	27.20–61.70
Ti	%	11	0.991	0.490	0.706	0.390–2.313
V	ppm	13	112.53	103.90	17.15	80.00–135.00
Cr	%	37	0.202	0.194	0.056	0.068–0.424
Mn	%	11	0.174	0.167	0.043	0.077–0.232
Fe	%	12	13.967	13.400	2.562	10.900–17.640
Co	%	33	0.004	0.004	0	0.003–0.005
Ni	%	16	0.013	0.009	0.011	0.002–0.034
Cu	ppm	4	15.58	9.95	10.79	8.20–34.20
Zn	ppm	7	10.03	5.80	9.07	2.20–30.50
Ga	ppm	14	5.56	5.22	1.16	4.10–7.41
Ge	ppm	5	0.15	0.19	0.09	0.03–0.24
As	ppm	2	1.01	1.01	0.93	0.08–1.94
Se	ppm	0	–	–	–	–
Br	ppm	1	0.10	0.10	0	0.10
Rb	ppm	12	2.66	1.90	1.69	0.78–5.30
Sr	ppm	39	134.41	126.00	67.25	70.00–530.00
Y	ppm	9	40.90	33.40	16.02	26.40–73.16
Zr	ppm	37	146.82	140.00	48.99	60.00–260.00
Nb	ppm	9	8.56	6.85	3.74	5.00–15.26
Mo	ppm	3	0.10	0.10	0.01	0.09–0.12
Ru	ppm	1	0.001	0.001	0	0.001
Rh	ppm	0	–	–	–	–
Pd	ppb	1	3.90	3.90	0	3.90
Ag	ppb	0	–	–	–	–
Cd	ppb	2	6.55	6.55	0.15	6.40–6.70
In	ppb	0	–	–	–	–
Sn	ppm	0	–	–	–	–
Sb	ppb	0	–	–	–	–
Te	ppb	0	–	–	–	–
I	ppm	1	3.00	3.00	0	3.00
Cs	ppb	13	64.77	70.00	25.79	20.00–100.00
Ba	ppm	39	122.29	91.70	65.00	48.47–371.00
La	ppm	39	9.85	10.60	3.30	4.69–15.30
Ce	ppm	39	26.25	29.90	8.77	12.28–39.60
Pr	ppb	5	3.56	3.48	1.18	1.82–5.14
Nd	ppm	39	16.54	16.00	6.18	8.10–28.00
Sm	ppm	39	5.42	6.31	2.18	2.38–8.89
Eu	ppm	39	1.04	1.02	0.21	0.66–1.41

Gd	ppm	10	5.25	4.75	2.35	2.88–10.18
Tb	ppm	39	1.23	1.22	0.54	0.52–2.03
Dy	ppm	15	5.30	4.70	2.46	3.15–11.80
Ho	ppm	10	1.20	0.95	0.62	0.66–2.43
Er	ppm	8	3.69	3.16	1.77	1.87–6.73
Tm	ppm	6	0.45	0.41	0.22	0.23–0.90
Yb	ppm	39	4.46	3.40	1.97	1.92–7.40
Lu	ppm	39	0.63	0.51	0.27	0.28–1.03
Hf	ppm	39	3.90	3.32	1.58	1.70–6.42
Ta	ppm	39	0.52	0.57	0.21	0.19–0.80
W	ppm	8	0.18	0.19	0.07	0.09–0.31
Re	ppb	5	0.28	0.21	0.25	0.01–0.61
Os	ppb	5	3.62	2.90	3.58	0.00009–9.30
Ir	ppb	11	5.74	5.60	4.18	0.10–12.00
Pt	ppm	1	0.01	0.01	0	0.01
Au	ppb	10	2.08	2.15	1.33	0.06–4.00
Hg	ppm	0	–	–	–	–
Tl	ppb	0	–	–	–	–
Pb	ppm	5	0.81	0.99	0.30	0.24–1.02
Bi	ppb	0	–	–	–	–
Th	ppm	39	1.44	1.21	0.60	0.51–2.39
U	ppm	38	0.38	0.36	0.14	0.17–0.67

Table A3. Characteristics of lunar gabbros in terms of the content of selected chemical elements based on chemical analyses of rocks obtained from lunar meteorites (authors' own work based on Koblitz, 2010)

	unit	**n**	**mean**	**median**	**deviation**	**range**
H	ppm	1	200	200	0	200
Li	ppm	0	–	–	–	–
Be	ppb	0	–	–	–	–
B	ppb	0	–	–	–	–
C	%	0	–	–	–	–
N	%	0	–	–	–	–
F	ppm	0	–	–	–	–
Na	%	8	0.224	0.209	0.076	0.100–0.370
Mg	%	7	3.597	3.740	0.296	2.980–3.870
Al	%	7	6.038	5.880	0.653	5.27–7.11
Si	%	6	20.963	21.350	1.152	18.70–22.00
P	%	2	0.075	0.075	0.053	0.022–0.127
S	%	2	0.335	0.335	0.145	0.190–0.480
Cl	ppm	0	–	–	–	–
K	%	9	0.043	0.033	0.025	0.020–0.108
Ca	%	6	8.352	8.485	0.773	6.87–9.47
Sc	ppm	16	91.36	94.05	19.69	24.40–112.60
Ti	%	6	1.598	1.390	0.848	0.911–3.433
V	ppm	4	76.25	80.00	15.37	53.00–92.00
Cr	%	13	0.196	0.185	0.097	0.075–0.507
Mn	%	7	0.237	0.262	0.048	0.139–0.283
Fe	%	9	17.182	17.100	1.374	14.200–19.300
Co	%	16	0.003	0.002	0.001	0.002–0.008
Ni	%	9	0.005	0.003	0.005	0.001–0.020
Cu	ppm	0	–	–	–	–
Zn	ppm	7	5.29	2.50	5.34	1.35–17.00
Ga	ppm	7	3.23	3.00	0.86	2.20–5.14
Ge	ppm	2	3.05	3.05	0.85	2.20–3.90
As	ppm	3	0.13	0.14	0.05	0.28–0.61
Se	ppm	3	0.41	0.35	0.14	0.28–0.61
Br	ppm	3	0.16	0.16	0.04	0.11–0.20
Rb	ppm	4	1.62	1.61	0.77	0.66–2.60
Sr	ppm	15	140.24	140.00	44.64	57.00–220.00
Y	ppm	1	22.30	22.30	0	22.30
Zr	ppm	9	107.67	97.00	50.35	45.00–190.00
Nb	ppm	0	–	–	–	–
Mo	ppm	0	–	–	–	–
Ru	ppm	0	–	–	–	–
Rh	ppm	0	–	–	–	–
Pd	ppb	0	–	–	–	–
Ag	ppb	2	35.83	35.83	28.17	7.66–64.00
Cd	ppb	3	7.87	6.70	3.25	4.60–12.30
In	ppb	2	1.30	1.30	0.58	0.72–1.88
Sn	ppm	0	–	–	–	–

Sb	ppb	3	20.75	3.14	24.93	3.11–56.00
Te	ppb	1	4.80	4.80	0	4.80
I	ppm	0	–	–	–	–
Cs	ppb	4	83.70	55.40	60.23	37.00–187.00
Ba	ppm	13	73.38	65.00	30.49	27.00–130.00
La	ppm	18	3.87	3.35	1.56	1.44–8.50
Ce	ppm	17	11.08	9.80	4.19	4.22–22.40
Pr	ppb	0	–	–	–	–
Nd	ppm	10	9.49	9.50	2.54	3.97–12.30
Sm	ppm	17	3.27	3.00	0.85	1.46–4.75
Eu	ppm	17	1.00	1.03	0.29	0.34–1.37
Gd	ppm	5	4.47	5.00	1.32	2.35–5.90
Tb	ppm	16	0.90	0.85	0.15	0.72–1.23
Dy	ppm	8	5.83	5.75	1.38	3.06–7.50
Ho	ppm	5	1.41	1.39	0.23	1.10–1.70
Er	ppm	1	2.17	2.17	0	2.17
Tm	ppm	3	0.63	0.70	0.15	0.42–0.77
Yb	ppm	17	3.75	3.57	0.73	2.28–5.08
Lu	ppm	17	0.56	0.54	0.11	0.36–0.82
Hf	ppm	16	2.62	2.48	0.46	2.06–3.35
Ta	ppm	16	0.36	0.35	0.07	0.22–0.50
W	ppm	3	0.13	0.10	0.05	0.08–0.20
Re	ppb	1	0.02	0.02	0	0.02
Os	ppb	1	380.00	380.00	0	380.00
Ir	ppb	6	61.22	2.95	112.65	0.30–310.00
Pt	ppm	0	–	–	–	–
Au	ppb	9	22.16	1.10	44.36	0.17–140.00
Hg	ppm	0	–	–	–	–
Tl	ppb	2	6.96	6.96	2.70	4.26–9.66
Pb	ppm	0	–	–	–	–
Bi	ppb	2	2.17	2.17	0.54	1.63–2.70
Th	ppm	16	0.56	0.45	0.25	0.31–1.31
U	ppm	10	0.14	0.13	0.06	0.09–0.28

Table A4. Occurrence of minerals with mining potential in selected types of rocks present on the Moon (based on Papike et al., 1991; Rubin, 1997; Rubin and Ma, 2017)

Mineral	Formula	Basalts	Anorthosites	KREEP	Breccias
chlorapatite	$Ca_5[Cl](PO_4)_3]$			+	+
chromite	$FeCr_2O_4$	+	+		+
zircon	$Zr[SiO_4]$			+	
ilmenite	$FeTiO_3$	+	+	+	+
kamacite	α–(FeNi)	+	+		+
taenite	γ–(FeNi)	+	+		+
troilite	FeS	+	+	+	+
ulvöspinel	$TiFe_2O_4$	+			+